Heliyon 10 (2024) e29385

Contents lists available at ScienceDirect

Heliyon

journal homepage: www.cell.com/heliyon

Research article

Impact of coconut kernel extract on carcinogen-induced skin cancer model: Oxidative stress, C-MYC proto-oncogene and tumor formation

Sorra Sandhya [a,b], Joyeeta Talukdar [a,b], Gayatri Gogoi [c], Kumar Saurav Dey [d], Bikul Das [b,e], Debabrat Baishya [a,*]

[a] Department of Bioengineering and Technology, Gauhati University, Guwahati, Assam, India
[b] Department of Cancer and Stem Cell Biology, KaviKrishna Laboratory, Indian Institute of Technology-Guwahati Research Park, Assam, India
[c] Department of Pathology, Assam Medical College and Hospital (AMCH), Assam, India
[d] Guwahati Biotech Park, Guwahati, Assam, India
[e] Department of Stem Cell and Infection, Thoreau Lab for Global Health, University of Massachusetts, Lowell, MA, USA

ARTICLE INFO

Keywords:
Skin squamous cell carcinoma (SCC)
Oxidative stress
c-MYC gene
Coconut karnel extract (CKE)
DMBA/TPA

ABSTRACT

This study aimed at analysing the effects of coconut (*Cocos nucifera* L.) kernel extract (CKE) on oxidative stress, C-MYC proto-oncogene, and tumour formation in a skin cancer model. Tumorigenesis was induced by dimethylbenz[a]anthracene (DMBA)/12-*O*-tetradecanoylphorbol-13-acetate (TPA). In vitro antioxidant activity of CKE was assessed using 2, 2-diphenyl-1-picrylhydrazyl (DPPH), hydrogen peroxide (H_2O_2), total phenolic and flavonoid content assays. CKE showed a higher antioxidant activity then ascorbic acid (*P < 0.05, ****P < 0.0001). HPLC and NMR study of the CKE revealed the presence of lauric acid (LA). Following the characterization of CKE, mice were randomly assigned to receive DMBA/TPA Induction and CKE treatment at different doses (50, 100, and 200 mg/kg) of body weight. LA 100 mg/kg of body weight used as standard. Significantly, the CKE200 and control groups' mice did not develop tumors; however, the CKE100 and CKE50 treated groups did develop tumors less frequently than the DMBA/TPA-treated mice. Histopathological analysis revealed that the epidermal layer in DMBA-induced mice was thicker and had squamous pearls along with a hyperplasia/dysplasia lesion, indicating skin squamous cell carcinoma (SCC), whereas the epidermal layers in CKE200-treated and control mice were normal. Additionally, the CKE treatment demonstrated a significant stimulatory effect on the activities of reactive oxygen species (ROS), glutathione (GSH), catalase (CAT), and superoxide dismutase (SOD), as well as an inhibitory effect on lipid peroxidase (*P < 0.05, **P < 0.01, ***P < 0.001, ****P < 0.0001) and c-MYC protein expression (*P < 0.05, **P < 0.01, ***P < 0.001, ****P < 0.0001). In conclusion, CKE prevents the growth of tumors on mouse skin by reducing oxidative stress and suppressing c-MYC overexpression brought on by DMBA/TPA induction. This makes it an effective dietary antioxidant with anti-tumor properties.

* Corresponding author. Department of Bioengineering and Technology, Gauhati University, Guwahati, 781 014, Assam, India.
E-mail address: drdbaishya@gmail.com (D. Baishya).

https://doi.org/10.1016/j.heliyon.2024.e29385
Received 6 January 2024; Received in revised form 7 April 2024; Accepted 7 April 2024
Available online 16 April 2024

1. Introduction

Skin cancer is the most common type of cancer in humans, with increasing incidence, morbidity, and mortality rates worldwide [1,2]. It can be broadly classified into two types: non-melanoma skin cancers (NMSC), which originate from cells derived from the epidermis, and melanoma cancer, which results from dysfunction of the melanocytes [2]. According to Global Cancer Statistics 2020, there are 1,198,073 incidences of NMSC and 63,731 deaths worldwide [1,3]. The most common types of NMSC among Caucasians are squamous cell carcinoma (SCC) and basal cell carcinoma (BCC) [1,4–7]. SCC accounts for 20 % of NMSC cases worldwide, while BCC accounts for 80 % [8]. However, NMSC incidence has increased by 3–8% annually since 1960, 18–20 times higher than melanoma [2,9,10]. Even compared to BCC, SCC is more common in the Indian subcontinent [11]. Therefore, there is a need to develop novel anti-cancer agents that can target SCC initiation and progression. According to current knowledge, the development of SCC is characterized by Deoxyribonucleic acid (DNA) damage brought on by ultraviolet (UV) radiation, which leads to an excessive proliferation of invasive squamous cells and metastasis [8,12,13]. Understanding the initial, promoting, and progressing stages of tumor formation is made possible by the use of animal models of carcinogen-induced skin cancer [14]. It has been demonstrated that 7,12-Dimethylbenz (a)anthracene (DMBA), a tumor initiating agent and 12-*O*-tetradecanoylphorbol-13-acetate (TPA), a tumor promoter are the most frequently used chemical carcinogens in chemically-induced skin cancer models [14–17]. These models induce two-stage sub-cutaneous skin carcinogenesis, which closely resembles human SCC [14–17]. This DMBA/TPA induced skin cancer model has been previously employed to generate novel anti-cancer agents such as salidroside, phospholipase Cepsilon and hesperidin [15,17,18]. Nevertheless, the mechanisms of action of these studies are restricted. In support of these studies, we also utilized DMBA/TPA induced skin cancer to investigate the anticancer activity of coconut (Cocos nucifera L.) kernel (CK) extract (CKE).

The coconut fruit's interior, or CK, is a food item with a high nutritional value and an abundance of vitamins, minerals, and fibre [19]. It belongs to the Arecaceae family. In India, the coconut tree is referred to as "Kalpavriksha" (the tree that gives everything) [19] and CK used as a traditional herbal medicine, offers numerous health benefits such as anti-aging, anti-bacterial, antifungal, antioxidant, and lipid reduction, making it a valuable tool for overall health [19,20]. Virgin Coconut Oil (VCO), extracted from CK by using traditional methods, exhibits high antioxidant properties and reduces oxidative stress by increasing catalase (CAT), superoxide dismutase (SOD), glutathione peroxidase (GPx) and glutathione reductase activity in cells [21–23]. It also shows anticancer properties against lung, liver and oral cancer cell lines [24–26]. Research also shows VCO's phenolic extract affects human hepatocellular carcinoma cells [27]. Additionally, it has been reported that VCO treated human neuroblastoma cells showed better mitochondrial health and reduced the release of reactive oxygen species (ROS), oxidative stress response genes, and inflammatory genes [28]. Moreover, its primary component, lauric acid (LA), also provided effective antioxidant activity within the cell, thereby providing cell protection and inhibited neuroinflammation [28]. Even, other study claimed that coconut oil's LA treatment kills human colon cancer cells by up to 93 % after 48 h of treatment by inducing oxidative stress and apoptosis in the cells [29]. More recent study also demonstrated that LA treatment prevents liver from ethanol-induced hepatotoxicity by reducing oxidative stress, inducing apoptosis and upregulating hepatocyte nuclear factor-4 alpha (HNF4α) [30]. However, the effect of coconut byproducts or LA alone on skin cancer is not well documented yet. Thus, an extensive investigation was conducted to better understand the anticancer effects of CKE on DMBA/TPA-induced skin cancer in relation to oxidative stress and c-MYC gene expression.

The c-MYC proto-oncogene, a key player in cancer development and progression, overexpression enhances pluripotency and tumorigenicity [31]. As with oxidative stress in cells, c-MYC plays a pivotal role in the development and metastasis of cancer [32]. Its regulation of cellular proliferation, differentiation, and apoptosis is disrupted by irregular expression, leading to aggressive growth behavior in cells, a phenomenon observed in human cancer, prompting researchers to target this gene for cancer treatment [33–39]. According to reports, the development of SSC is facilitated by the activation of proto-oncogenes such as over-expression of c-MYC and/or the inactivation of tumor suppressor genes like p53 mutation in keratinocytes of both animal and human skin [34,40–43]. According to our earlier study, a c-MYC can increase the cancer stemness of cancer stem cells (CSCs) by controlling the HIF-2α stemness pathway through NANOG and SOX2 [44]. Another study indicated that when c-MYC is activated, normal cells experience apoptosis with restricted growth factors, but tumor cells are resistant to c-MYC's apoptotic effects [45]. Furthermore, overexpression of the c-MYC gene during the carcinogenesis process promotes gene amplification in normal cells, which increases the proliferation of cancer cells commonly seen in human cancer [34,46]. More significantly, ROS production and DNA damage in cells are also induced by c-MYC [47,48]. According to Graves et al. (2009), the regulation of ROS homeostasis is dependent on c-MYC activity [48]. These investigations therefore suggested that c-MYC is crucial for increasing oxidative stress in cells as cancer progresses. However, it is unknown, whether CKE affects c-MYC-induced oxidative stress in skin cancer. Therefore, in this study we investigated the effects of CKE on oxidative stress, the c-MYC proto-oncogene, and tumour formation using a SCC skin cancer model induced by DMBA/TPA. Our goal was to provide non-toxic dietary product as chemopreventive options for the clinical treatment of NMSC.

Here we report that CKE delays or inhibits skin cancer in mice by acting as potent a potent dietary antioxidant that boosts the activities of glutathione (GSH), CAT, SOD, and reduces ROS and lipid peroxidase (MDA). By decreasing the overexpression of the c-MYC protein, CKE may also act as a c-MYC-mediated oxidative stress inhibitor. Our study also reveals c-MYC-mediated oxidative stress mechanism in DMBA/TPA induced skin cancer. Thus, CKE therefore functions as potent anticancer drug against DMBA/TPA induced skin cancer.

2. Materials and methods

2.1. Reagents and kits

DMBA, TPA, Thiobarbituric acid (TBA), Trichloroacetic acid (TCA), Lauric acid, Acetic acid, Sodium dodecyl sulphate (SDS), *N*-butanol-pyridine, 5,5′-dithiobis (2-nitrobenzoic acid) (DTNB), L-Glutathione, reduced (GR), β-NADPH (#N-1630-Sigma-Aldrich), Hydrogen peroxide (H_2O_2), Phosphate buffer, Bradford Reagent and Bovine Serum Albumin (BSA), Paraffin, 40 % formalin, Hematoxylin & Eosin (H&E) Reagents were purchased from Sigma-Aldrich Co. (Mumbai, India). Superoxide Dismutase (SOD) Activity Assay Kit and DPPH (2, 2-diphenyl-1-picrylhydrazyl) Antioxidant Assay Kit were purchased from abcam, Mumbai India. The Super sensitive TM Polymer-HRP IHC Detection system and ready-to-use antibody of anti-*c*-MYC protein [9E10] (#AM318-M) was acquired from BioGenex, CA, USA.

2.2. Collection and preparation of coconut kernel

The coconut fruits were gathered from Gauhati University's botanical garden in Guwahati, Assam. Botanical Survey of India (BSI) in Shillong, Meghalaya, India, completed the identification and authentication (BSI/ERC/2015/Plant identification/806). Using a scrapper, 2–3 coconut kernels were then removed, and they were freeze-dried for a further 20–25 days at 4°C.

2.3. High performance liquid chromatography (HPLC) analysis

The sample preparation procedure was simple [49,50]. A 1.0 g of CKE was combined with 1 ml of HPLC-grade methanol that was purchased from the Merck company in Mumbai, India. Next, a 0.45 μm filter was used to filter the mixture. The standard graph of LA was obtained using pure LA (Merck, Mumbai, India).

The Agilent 1260 Infinity HPLC (analytical) system was utilized to ascertain the Lauric acid content in CKE. The apparatus consisted of an SPD-10Avp ultraviolet detector, an LC-10ADvp pump, a SIL-10ADvp auto sampler, a DGU-14A degasser, and a SCL-10Avp system controller. The stationary C18 column was operated at room temperature. The mobile phase was HPLC-grade methanol, flowing at a rate of 0.5 ml/min. The injection volume for every chromatographic run was 50 μl. A wavelength of 203 nm was used for the detection process. Next, we used the Agilent 1260 Infinity HPLC (preparative) system under the same conditions to isolate the targeted peak that we had obtained from CKE. The HPLC analysis was performed under the supervision of Guwahati Biotech Park, Guwahati, Assam.

2.4. Nuclear magnetic resonance (NMR)

To identification and structural analysis of isolated targeted compound from CKE in liquid phase was characterized by ^{1}H NMR and ^{13}C NMR using 400 MHz Varian MercuryPlus NMR Spectrometer under the supervision of Sophisticated Central Instruments Facility, Indian Institute of Technology (IIT) Guwahati, Assam. The instrument is equipped with Oxford superconducting magnet of frequency 400 MHz (9.4 T) with probe capacity of 5 mm 1H 13C/X and Mercury 400 high resolution NMR console.

2.5. DPPH free radical scavenging assay

The anti-oxidant activities of CKE on DPPH were measured using previously described method [51–53]. The absorbance was measured at 517 nm. Each test was run in triplicate, and the following equation [54] was used to determine the percentage of DPPH Scavenging activity:

$$\text{DPPH Scavenging Activity}(\%) = \frac{\text{Control Absorbance} - \text{Test Absorbance}}{\text{Control Absorbance}} \text{x}100 \quad \text{(i)}$$

2.6. H_2O_2 free radical scavenging assay

The antioxidant activities of CKE on H_2O_2 were determined by using previous method [51,53,55]. The absorbance was measured at 230 nm. Each test was run in triplicate, and the following equation [56] was used to determine the percentage of H_2O_2 Scavenging activity:

$$\text{Hydrogen Peroxide Scavenging Activity}(\%) = \frac{\text{Control Absorbance} - \text{Test Absorbance}}{\text{Control Absorbance}} \text{x}100 \quad \text{(ii)}$$

2.7. Calculation of IC_{50} value

The average percent of scavenging capacity was determined through the use of linear regression plots for IC_{50} values, where the ordinate denotes the average percent of scavenging capacity and the abscissa denotes the concentration of the tested plant extracts. The amount of sample needed to scavenge 50 % of H_2O_2 (IC_{50} H_2O_2) and 50 % of DPPH (IC_{50} DPPH) was then calculated.

2.8. Total phenolic content (TPC)

The Folin-Ciocalteau reagent was used to estimate the TPC of the CKE, as previously described [57]. Briefly, 80 % methanol was used to dissolve 1 mg of CKE. A mixture of 1500 μl freshly prepared Folin-Ciocalteu regent and 300 μl CKE solution was combined. After that, 1300 μl of 7.5 % Na2CO3 was added to the mixture, and it was left to stand at room temperature for 30 min in the dark. The absorbance was measured at 760 nm. Each test was run in triplicate and the TPC was expressed as mg of gallic acid equivalent (GAE) per 1 g of CKE [58].

2.9. Total flavonoid content (TFC)

The TFC of CKE was analyzed by the method described by Adekola et al., 2017 with slight modification [58]. Briefly, ethanol was used to dissolve 1 mg of CKE. After that, 500 μl of CKE solution was combined with 30 μl of 5 % NaNO2. After 5 min, 300 μl of 10 % AlCl3 was added and mixed. Following an additional 5 min, 200 μl of 1 N NaOH was combined with. The absorbance was measured at

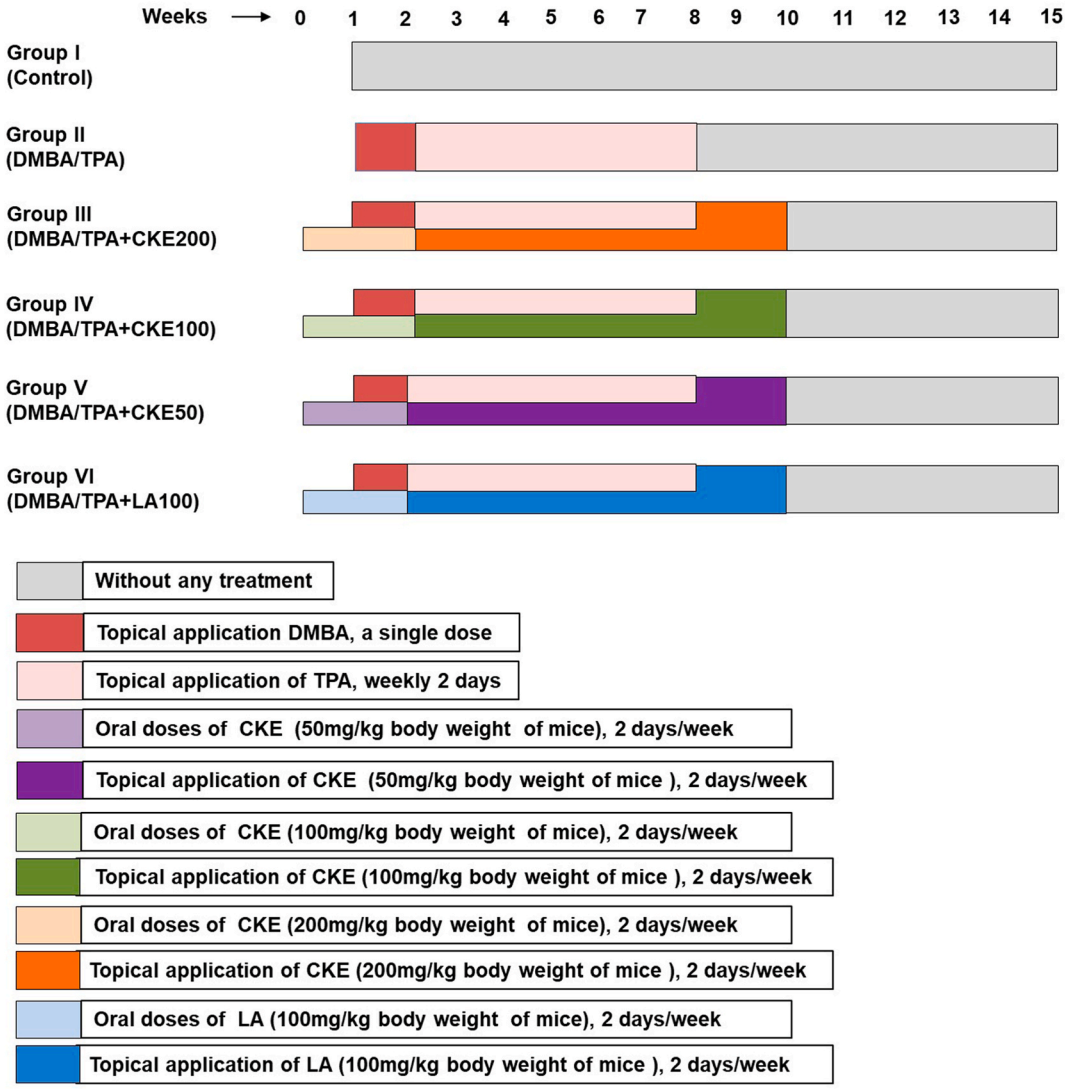

Fig. 1. Schematic illustration of the in vivo experimental plan to assess the anticancer potential of CKE treatment in a model of skin squamous cell carcinoma (SCC) induced by DMBA/TPA. Serving as the control group, Group I mice were fed a regular diet and did not receive any medical attention. A single topical dose of 400 nm DMBA was administered to Group II, Group III, Group IV, Group V and Group VI mice. One week after the DMBA induction, multiple topical applications of 5 nmol TPA were applied. In addition, CKE200 (200 mg/kg body weight), CKE100 (100 mg/kg body weight), CKE50 (50 mg/kg body weight), and LA100 (100 mg/kg body weight) were administered weekly to Group III, Group IV, Group V, and Group VI mice that served as treatment groups. The treatments began 1 week before the tumour initiation process and continued for ten weeks.

515 nm. Each test was run in triplicate and the TFC was expressed as mg of quercetin equivalent (QE) per 1 g of CKE [58].

2.10. Animals and treatments

Eight to nine-weeks-old Swiss albino mice, *Mus musculus*, were obtained from Zoology Department, Gauhati University, Assam, India and kept in well-ventilated polypropylene cages under germ-free condition with a 12 h light and dark cycle. All Protocols for animal experimentation were approved by the Institutional Animal Ethics Committee, (IAEC) at Gauhati University (IAEC/PER/2014–2015/02). Five groups of mice were randomly assigned. For every group, ten mice. Fig. 1 depicts the in vivo study's experimental design. By employing the cutaneous two-stage skin carcinogenesis protocol as previously mentioned [59,60], skin cancer was induced in mice. In brief, after three days of shaving the mice's backs, a single dose of 400 nmol DMBA was applied topically to initiate the tumor. One week later, the mice received multiple topical applications of 5 nmol TPA twice a week up to eight weeks. Mice in Group I (control) were fed a regular diet in the absence of any medication. The mice in Group II (DMBA/TPA) were solely given DMBA/TPA induction. In addition to DMBA/TPA induction, Group III (CKE200), Group IV (CKE100), Group V (CKE50); additionally received a dose of 200, 100, and 50 mg CKE/kg body weight, respectively, prior to 30 min before TPA application until 10 weeks. Group VI (LA100) also received DMBA/TPA induction similar to Group II, but in addition they received a dose 100 mg LA/kg body weight. LA treatment was used as positive control for CKE. Each week, the body weights and counts of skin tumors (>1 mm) in each animal were recorded. By cervical dislocation, all grouped animals were sacrificed at the conclusion of the experiment for histopathology, immunohistochemistry, and biochemical analyses [61].

2.11. Histopathology analysis

The skin and tumor tissue were embedded in paraffin blocks after being fixed for 24–48 h in 10 % neutral buffered formalin [10 % formalin +90 % distilled water + 9 g sodium chloride (NaCl) + 12 g sodium phosphate (Na_2HPO_4)] [62]. Using a microtome (Model: LEICA RM2245), sections with a thickness of 5.0 μm were cut and then stained with H&E.

2.12. Immunohistochemistry (IHC) analysis

IHC was done using a Super sensitive ^{TM}Polymer-HRP IHC Detection system kit, according to manufacturer's instructions [44,63]. Mouse c-MYC antibody (Santa Cruz Biotechnology) was used in 1:100 dilution.

2.13. RNA extraction and real time qPCR assay

Total RNA extraction from skin/tumor tissue were performed using the RNeasy Mini Kit (Qiagen #74106), followed by cDNA isolation using the Sensiscript RT Kit (Qiagen: 205213). The nano-drop UV spectrophotometer was utilized to confirm the purity of the RNA samples by measuring 260nm/280 nm ratios. Next, using TaqMan Gene Expression Assays (Applied Biosystems, Foster City, CA, http://www.appliedbiosystems.com), real-time quantitative reverse transcription-polymerase chain reaction (qPCR) was carried out at 50 cycles using 2 ng of starting cDNA. Briefly, the RNA levels were calibrated using the ΔΔCT method using SDS software, version 2.2.1 (Applied Biosystems, Foster City, USA) as described [44,64]. The RNA levels were normalized to GAPDH as an endogenous control. We used the MYC (Mm01224449_m1) and GAPDH (Mm99999915_g1) mouseTaqMan Gene Expression primers [51].

2.14. Oxidative stress analysis

To assess the antioxidant potential of CKE in DMBA/TPA induced mice, we measured the levels of ROS, MDA, GSH, SOD, and CAT in the skin, tumour, and liver tissue obtained from mice of all groups at the end of the experiments (15 weeks). Antioxidant enzyme activity in tissues is analyzed using GSH, SOD, and CAT, while ROS and MDA serves as an indicator for oxidative stress analyses. PBS phosphate buffer saline (PBS-pH 7) containing 2 % foetal bovine serum (FBS) (#RM9954 – Hi Media Laboratories Pvt. Ltd, Mumbai, India) was used to thoroughly wash every sample. 10 % tissue homogenate (w/v) from a portion of the sample was prepared using a lysis buffer (pH 6.7) containing 50 mM sodium phosphate (Na2HPO4) and 1 mM ethylene-diamine-tetraacetic acid (EDTA) (#E9884-Sigma Aldrich) in a biosafety cabinet (#1300 Series Class II, Type A2, Thermo Fisher, USA). The homogenate was then centrifuged at 12000g for 15 min. Thus, the supernatant was collected for protein, ROS, MDA, GSH, SOD, and CAT estimation.

2.14.1. Protein estimation

The Bradford assay was used to estimate the protein content of 10 % tissue homogenate using BSA as a standard as described [65]. Briefly, 0.1 ml of prepared tissue homogenate was mixed with 3 ml of standard Bradford reagent. Incubated for 40–45 min at room temperature after gently mixing with a vortex. The absorbance was measured at 595 nm.

2.14.2. Measurement of reactive oxygen species (ROS) activity

The ROS activity was estimated using an ELISA kit in accordance with manufacturer instructions of sigma aldrish as described previously [66]. Briefly, the fresh tissue homogenate was centrifuged for 20 min at 3000RPM, collected, and analyzed for ROS levels. The relative fluorescence unit (RFU) was measured after 30 min by using Gemini Spectra MAX microplate reader (Molecular Devices, Sunnyvale, CA [67].

2.14.3. Lipid peroxide (MDA) assay

Estimation of lipid peroxidase level in 10 % tissue homogenate were calculated according to method describe by Ohkawa et al., 1979 & Dhawan et al., 1999 [68,69]. Briefly, a mixture of 0.1 % SDS, 20 % acetic acid, and 0.8 % TBA solution was added to 100 μl of prepared 10 % tissue homogenate. 100 μl of prepared 10 % tissue homogenate added in a mixture of 0.1 % SDS, 20 % acetic acid and 0.8%TBA solution. After heating for 30–35 min, this mixture was cooled and separated using an N-butanol-pyridine mixture. The absorbance was recorded at 532 nm and content of MDA was expressed as nmol/mg protein.

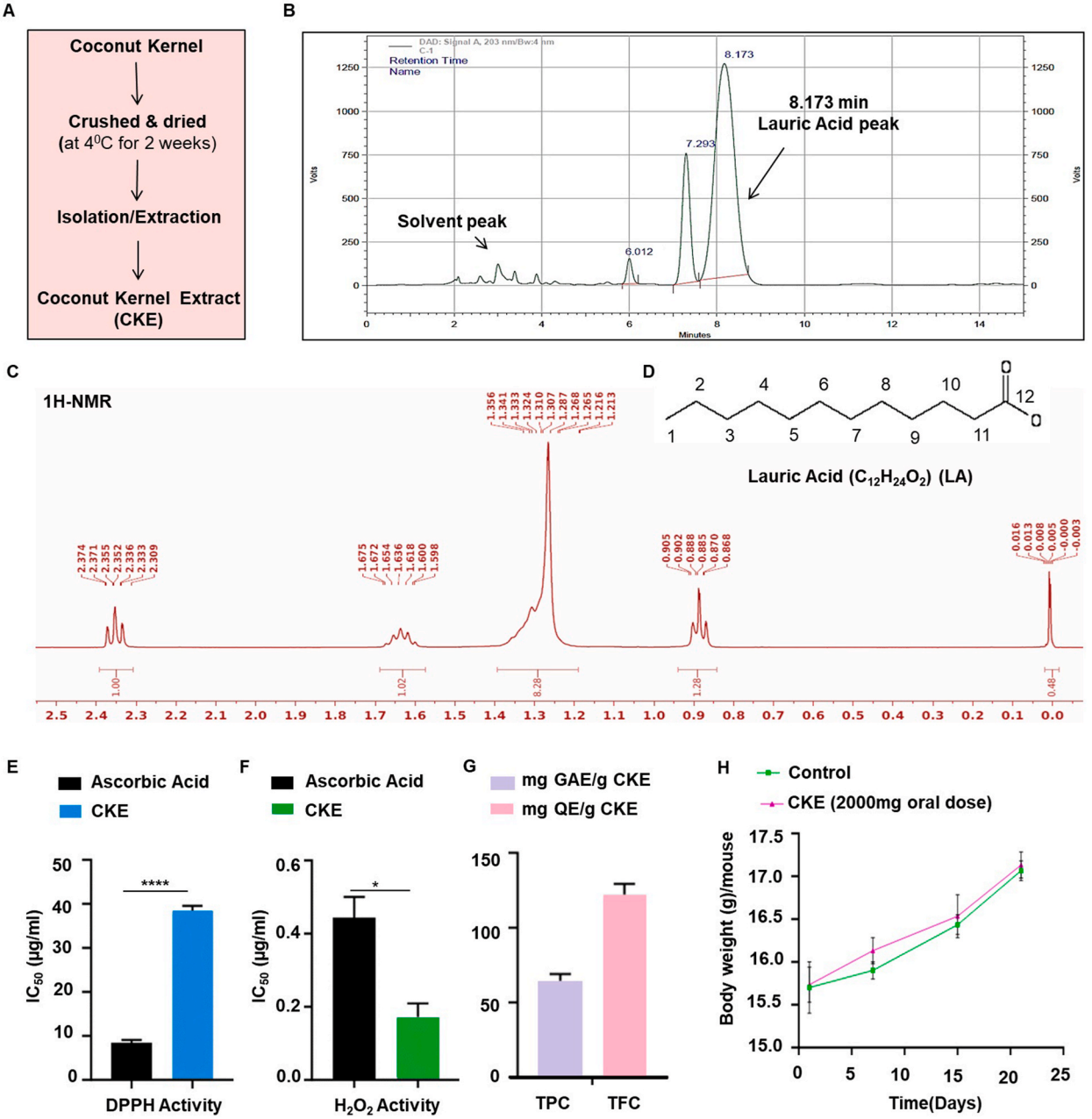

Fig. 2. Isolation and characterization of Coconut Kernel Extract (CKE). A. Standard Process of Isolating CKE from Coconut Kernel. **B.** HPLC chromatogram showing largest peak of lauric acid (LA) at 8.1 73 min as compared to standard peaks of pure LA at wavelength 203 nm. **C.** 1H NMR spectrum of LA. **D.** Chemical structure of LA. **E & F.** Bar diagram showing IC_{50} value of CKE against DPPH activity and H_2O_2 activity in comparison to ascorbic acid. G. Bar diagram showing total phenolic content (TPC) equivalent to gallic acid (GAE) and total flavonoid content equivalent to quercetin (QE) in CKE. H. Line graph showing the mice's body weight over the course of an acute oral toxicity study, spanning 21 days. Data are expressed as mean (N = 3) ± Standard error of mean (SEM), *p < 0.05, ****p < 0.0001, *t*-test.

2.14.4. Catalase activity (CAT) assay

The Catalase activity was estimated using the procedure outlined in Aebi (1984) [70]. Following the addition of 100 μl of prepared 10 % tissue homogenate to 50 mM phosphate buffer (pH 7), 30 mM solution of H_2O_2 was added to the mixture. After adding H_2O_2, the absorbance was measured at 240 nm in less than 2 min. The activity of the enzyme was expressed as μmol of H_2O_2 reduced/mg protein/minute.

2.14.5. Glutathione (GSH) assay

The method of Daniela et al., 1660 was slightly modified to estimate the glutathione level [71]. 100 μl of 10 % tissue homogenate was added to a mixture containing 0.925 ml of phosphate buffer, 5 μl of DTNB, 20 μl of TCA, 20 μl of NADPH, and 20 μl of GR. The absorbance was measured at 412 nm as soon as the samples were added. The GSH level was expressed as nmol/mg of protein.

2.14.6. Superoxide dismutase (SOD) assay

The superoxide dismutase activity was estimated according to manufacturer instructions using the SOD determination kit (#19160-sigma Aldrich). The absorbance was measured at 450 nm. The SOD level was expressed as unit per mg (U/mg) of protein with U/mg of protein, with one unit of the enzyme equal to the quantity needed to inhibit 50 % of SOD activity.

2.15. Statistical analysis

The statistical analysis was performed using GraphPad Prism 10.0 (Hearne Scientific Software, Chicago, IL, USA). The significance of the difference in groups was analyzed using one-way analysis of variance (ANOVA) with the Dunnett post hoc test. *t*-test was used for in vitro antioxidant capacity comparison. Additionally, correlation analysis in between antioxidant activity with TPC and TFC were expressed as Pearson correlation co-efficient. Data are expressed as means ± SEM (*P < 0.05, **P < 0.01, ***P < 0.001, and ****P < 0.0001).

3. Results

3.1. Isolation and characterization of coconut kernel extract (CKE)

Fig. 2A shows the standard process of isolating CKE from CK. In brief, the CK was scraped with a scrapper and freeze dried at 4°C for 20–25 days. Following that, dried CK was used to extract CKE continuously for three days, 6 h a day, using a soxhlet apparatus. CKE was obtained as thick, colourless wax or oil after evaporation, and it was then stored at 20°C. The sample was immediately characterized by HPLC analysis following the acquisition of CKE. The findings show that CKE at wavelength 203 nm has three distinct peaks at retention times of 8.173, 7.293, and 6.012 min (Fig. 2B). The highest peak, which had a retention time of 8.173 min, was relatively near to the standard LA retention time of 8.123 min, out of three peaks (Supplementary Fig. 1A). Studies have previously indicated that 48–53 % LA is present in coconut oil, which validates our findings [28,72,73]. Thus, in order to verify the presence of LA in CKE, we separated the compound using a preparative HPLC column at retention time 8.173 min and subjected to ^{1}H (Figs. 2C) and ^{13}C NMR (Supplementary Fig. 2D) characterization. The isolated compound was identified as LA based on the results (Fig. 2D). However, we were unable to locate the remaining peaks depicted in Fig. 2B.

Furthermore, CKE samples were put through assays for the free radical scavengers DPPH and H_2O_2 assays in order to evaluate the

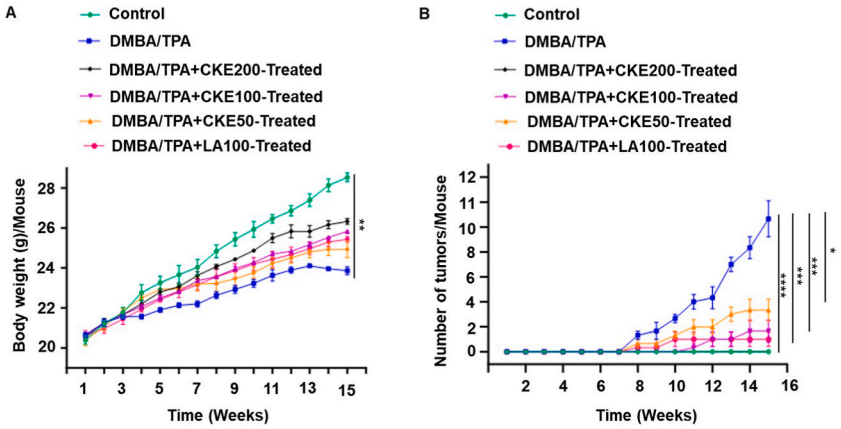

Fig. 3. Average body weight and tumor formation in response to CKE treatment in DMBA/TPA induced skin cancer model. A. A representative graph showing the mice's weekly body weights for each group over a period of 15 weeks. **B.** A representative graph displaying the total number of tumors observed in each group of mice over a period of 15 weeks. Data are expressed as mean (N = 8) ± Standard error of mean (SEM), *p < 0.05, **p < 0.01, ***p < 0.001, ****p < 0.0001, one way ANOVA analysis.

antioxidant potential of CKE in vitro [51]. Additionally, total phenolic content (TPC), and total flavonoid content (TFC) also measured in CKE [57,58]. Our findings demonstrated that in comparison to ascorbic acid, the CKE demonstrated a high IC_{50} value (38.41 ± 4.32; ****P < 0.0001) against DPPH (Fig. 2E) and a low IC_{50} value (0.171 ± 0.03; *P < 0.05) against H_2O_2 (Fig. 2F). CKE also showed high TPC (64.29 ± 4.32 mg GAE/g of CKE) and TFC (122.67 ± 7.15 mg QE/g of CKE) (Fig. 2G), indicating a higher potential for antioxidants. Even, Pearson correlation analysis suggested a strong positive correlation between antioxidant activity of CKE with TPC (DPPH, $R^2 = 0.87$; H_2O_2, $R^2 = 0.68$) and TFC (DPPH, $R^2 = 0.77$; H_2O_2, $R^2 = 0.77$). Our findings are consistent with earlier research showing a co-relation between antioxidant activity and phenolic and flavonoid compounds in a number of locally produced herbal extracts [74] and coconut fruit extract [75]. Additionally, we looked into the acute oral toxicity effect of CKE in accordance with the acute oral toxicity OECD/OCED (423) guidelines in order to assess the maximum dose limit of CKE in vivo [51,76]. CKE treated mice did not exhibit any physical symptoms associated with toxicity, such as breathing difficulties, gasping, writhing, palpitations, or death, nor did they show significant changes in body weight in comparison to the control group (****p < 0.00001) (Fig. 2G). Therefore, 200 mg/kg of mice's body weight, or a 1:10 ratio of 2000 mg oral dose, was determined to be the maximum CKE dosage for an in vivo study.

3.2. CKE significantly maintains body weight and inhibits or delays the tumor formation in DMBA/TPA induced mice

Over a 15-week period, we tracked the body weights and tumor formation of each group of mice in order to investigate the impact of CKE on the DMBA/TPA induced mice. As demonstrated by Fig. 3A, CKE significantly aids mice in maintaining body weight in a dose-dependent manner against DMBA/TPA induction. On the other hand, mice that were given DMBA/TPA without receiving any treatment exhibited a notable reduction in body weight in comparison to control group (**P < 0.01). Remarkably, mice in the control and CKE200 treated groups did not exhibit any tumor formation until the end of the experiment, whereas mice in the DMBA/TPA, CKE50, and CKE100 treated groups did exhibit tumor formation (*P < 0.05, **P < 0.01, ***P < 0.001, ****P < 0.0001) (Fig. 3B & Supplementary Fig. 2). Nonetheless, compared to mice given DMBA/TPA, fewer tumors were found in the CKE100, CKE50 and LA100 treated groups. Importantly, our findings indicated that LA100-treated group mice are more comparable to mice in the CK200-treated group. Out of the eight mice treated with LA100, we found that only one had two tumors formed. Additionally, concluded that when the rate of tumor growth increased, mice's body weight decreased.

Subsequently, we conducted a histopathological examination of skin and skin tumor samples from each mouse group to verify if CKE treatment prevents or delays the formation of tumors in mice. In both control and CKE200-treated mice, the normal squamous

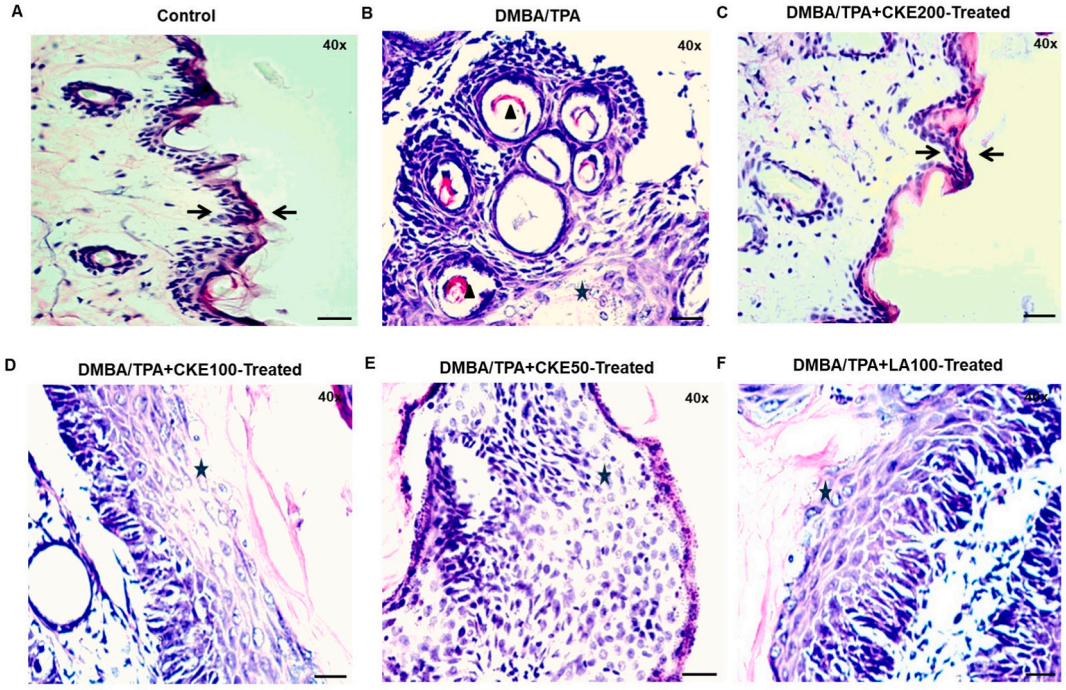

Fig. 4. Histopathology of skin/tumors at the end of 15 weeks in different treatment groups (40× magnification). A & C. Images showing the normal skin histoarchitecture of the control and CKE200 treated groups, respectively. The region between two arrow signs showing a well-defined epidermis, the underlying dermis, and subcutaneous tissue. **B.** Aberrant histoarchitecture displaying thickness of epidermal layer, triangle sign showing well-differentiated squamous papilloma with hollow centered squamous keratin pearl, and star sign indicating dysplastic lesions in DMBA/TPA induced mice. **D-F.** Skin histoarchitecture in the CKE100, CKE50, and LA100 treated groups showing corrugated epidermis with hyper-proliferative indicated by star sign and well-developed papilloma. Scale bar-20 μm.

epithelial cells and epidermal layers were readily apparent (Fig. 4A & C). Mice treated with DMBA/TPA, CKE100, CKE50, and LA100 showed clear signs of necrotic keratinocytes and characteristic squamous pearls with hyperplasia/dysplasia in some squamous epithelial cells located in the dermis (Fig. 4B, D, 4E & 4F). The development of dysplastic squamous epithelial cells will eventually result in an invasive form of squamous cell carcinoma, as demonstrated by the full thickness keratinocyte dysplastic squamous epithelial cells with atypical nuclei in DMBA/TPA induced mice at 20 weeks (Supplementary Fig. 3).

3.3. CKE significantly reduces oxidative stress in DMBA/TPA induced mice

In a biological system, oxidative stress is caused by ROS like superoxide radical (O2−), hydroxyl radical (OH), and H_2O_2, which ultimately damage DNA and cause cell necrosis or apoptosis [77]. Therefore, the one factor that may be in charge of disrupting cellular signalling during a body's normal mechanism is oxidative stress within the cell. Thus, in order to study oxidative stress and antioxidant enzyme activity, we measured the activity of ROS, MDA, GSH, CAT and SOD in liver and skin/tumor tissue that were taken from CKE-treated groups as well as control, LA100-treated and DMBA/TPA-induced groups [78]. It was observed that the ROS level in the skin/tumor (****$p < 0.0001$) and liver (****$p < 0.0001$) were significantly higher in DMBA/TPA induced mice in comparison to control, CKE200 and LA100 treated mice. The significant lower ROS level was observed in CKE200 treated mice compared to CKE100 (**$p < 0.01$) and CKE 50 (****$p < 0.0001$) treated mice (Figs. 5A & 6A). MDA level (**$p < 0.01$, ****$p < 0.0001$) in the mice treated with DMBA/TPA was significantly higher than that of the control and CKE-treated mice (Figs. 5B & 6B), suggesting an inhibitory effect. Conversely, a noteworthy rise in GSH levels (***$p < 0.001$, ****$p < 0.0001$)) was noted in mice treated with CKE200, CKE100, CKE50 and LA100 when compared to control and DMBA/TPA-induced mice (Figs. 5C & 6C), suggesting a possible antioxidant effect of CKE. Comparing CKE200, CKE100, and CKE50 treated groups to DMBA/TPA-induced mice, however, dose-dependently higher levels of GSH (***$p < 0.001$, ****$p < 0.0001$) were observed. Similarly, CAT (****$p < 0.0001$; Figs. 5D & 6D) and SOD (****$p < 0.0001$; Figs. 5E & 6E) levels were significantly higher in the CKE treated groups compared to the DMBA/TPA induced group. These results thus indicated that CKE decreases reactive oxygen species generation and lipid peroxidase, and increases glutathione, catalase, and superoxide dismutase activity to reduce oxidative stress in DMBA/TPA-induced mice.

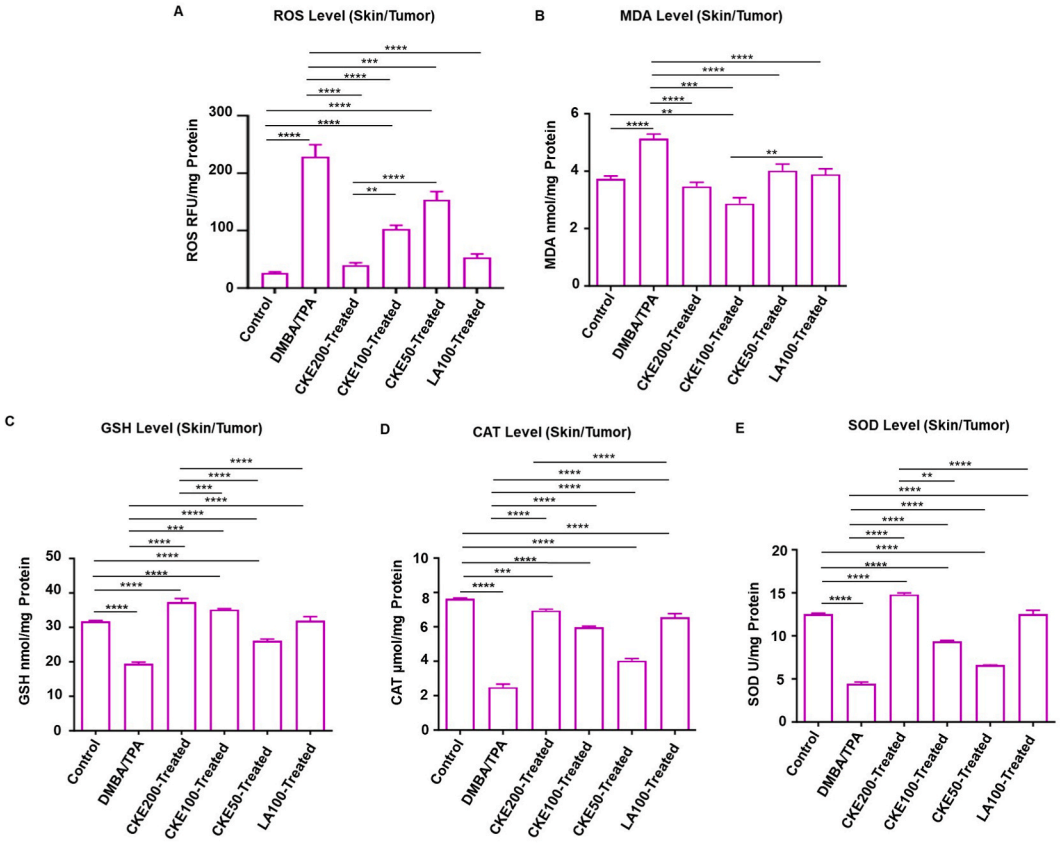

Fig. 5. Oxidative stress analysis in skin/tumor. A-D. The Bar Diagram showing comparative ROS, MDA, GSH, CAT and SOD level in the Skin/tumor tissue obtained from each grouped mice at the end of the experiment. Data are expressed as mean (N = 8) ± Standard error of mean (SEM), *$p < 0.05$, **$p < 0.01$, ***$p < 0.001$, ****$p < 0.0001$, one-way ANOVA analysis.

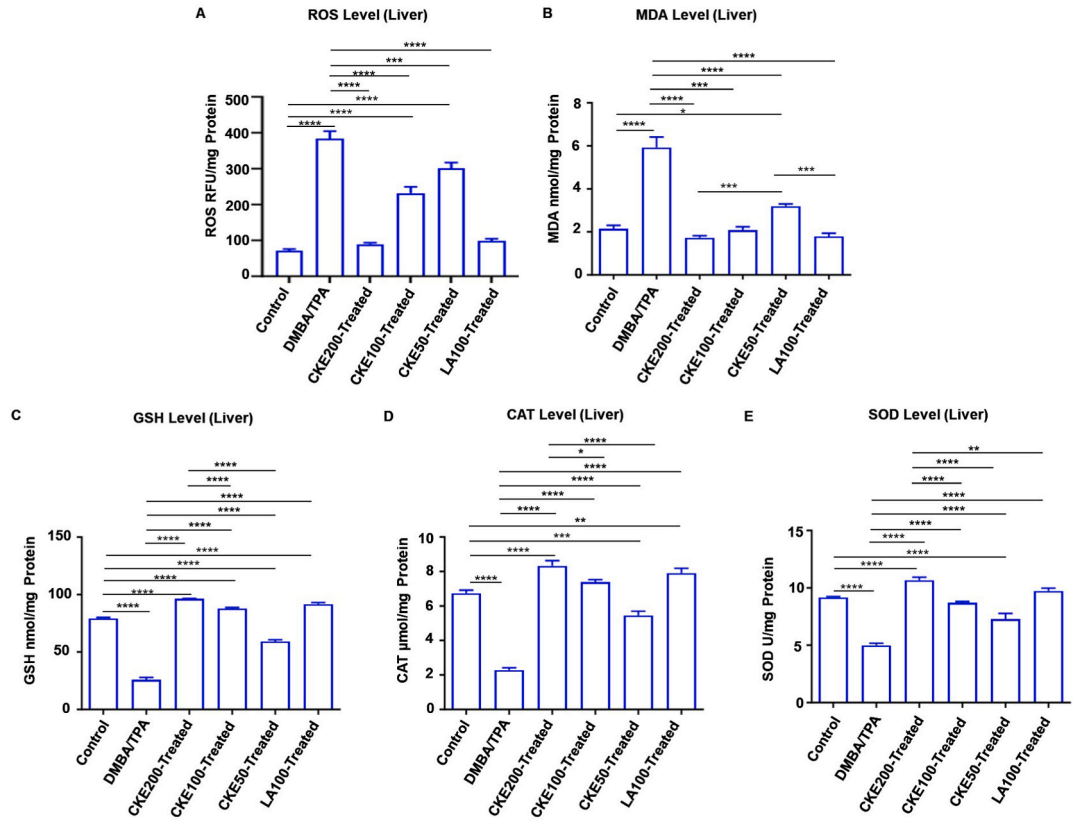

Fig. 6. Oxidative Stress Analysis in Liver. A-D. The Bar Diagram showing comparative ROS, MDA, GSH, CAT and SOD level in the liver tissue obtained from each grouped mice at the end of the experiment. Data are expressed as mean (N = 8) ± Standard error of mean (SEM), *p < 0.05, **p < 0.01, ***p < 0.001, ****p < 0.0001, one-way ANOVA analysis.

3.4. C-MYC inhibitory effect of CKE in DMBA/TPA induced mice

Proto-oncogene c-MYC modulates or controls a number of transcriptional pathways in cells, including angiogenesis, stem cell differentiation, apoptosis/survival, cell division, and immortalization [42]. However, it has been consistently noted that the majority of human cancers exhibit aberrant or excessive c-MYC gene expression, suggesting that c-MYC is a key player in the cancer progression [79–81]. Thus, in order to examine the impact of CKE on c-MYC protein expression, we used unstained histopathological slides for IHC staining in accordance with the manufacturer's instructions. We found that the majority of blue colour cells in the control (Fig. 7A) and CKE200-treated (Fig. 7C) groups of mice indicated negative staining of c-MYC protein expression. But in the grouped mice treated with DMBA/TPA (Fig. 7B), CKE100 (Fig. 7D), CKE50 (Fig. 7E), and LA100 (Fig. 7F) there were strong brown colour cells appeared that suggested positive c-MYC protein expression. Fig. 7G illustrated the quantification plot of c-MYC IHC score based on percentage of positive (brown) cells of each grouped mice. The significant decreased IHC score was observed in Control (****p < 0.0001) and CKE200 (****p < 0.0001) treated mice as compare to DMBA/TPA induced mice. Similarly, qPCR data confirms the significant increased c-MYC relative RNA levels in DBMA/TPA (***p < 0.001), CKE100 (**p < 0.01), CKE50 (**p < 0.01) and LA100 (*p < 0.05) treated mice as compare to CKE200 treated mice (Fig. 7H). Therefore, we deduced that CKE might have an inhibitory effect on the c-MYC gene; however, since CKE50 and CKE100 treated mice expressed the c-MYC gene positively (Fig. 7D & E), the dosage of CKE should be increased to inhibit the c-MYC gene.

4. Discussion

The study aimed to investigate the anti-cancer activity of CKE against DMBA/TPA-induced skin SCC by protecting cellular mechanisms like reducing oxidative stress and suppressing c-MYC gene expression. SSC, a subtype of NMSC, is the second most prevalent cancer in the world and is distinguished by abnormal keratinocyte proliferation [2,82]. More significantly, the Indian subcontinent has a higher prevalence of SCC [11]. The DMBA/TPA-inducing mouse model of skin cancer undergoes three phases of tumor formation: initiation, promotion, and progression, resulting from a specific mutation in the H-ras oncogene [61,83]. Therefore, studying the impact of CKE on the development of skin cancer will be greatly aided by the DMBA/TPA-induces model. In the current scenario, synthetic chemotherapeutic drugs are expensive, have side effects, and can cause multiple organ toxicity, leading to

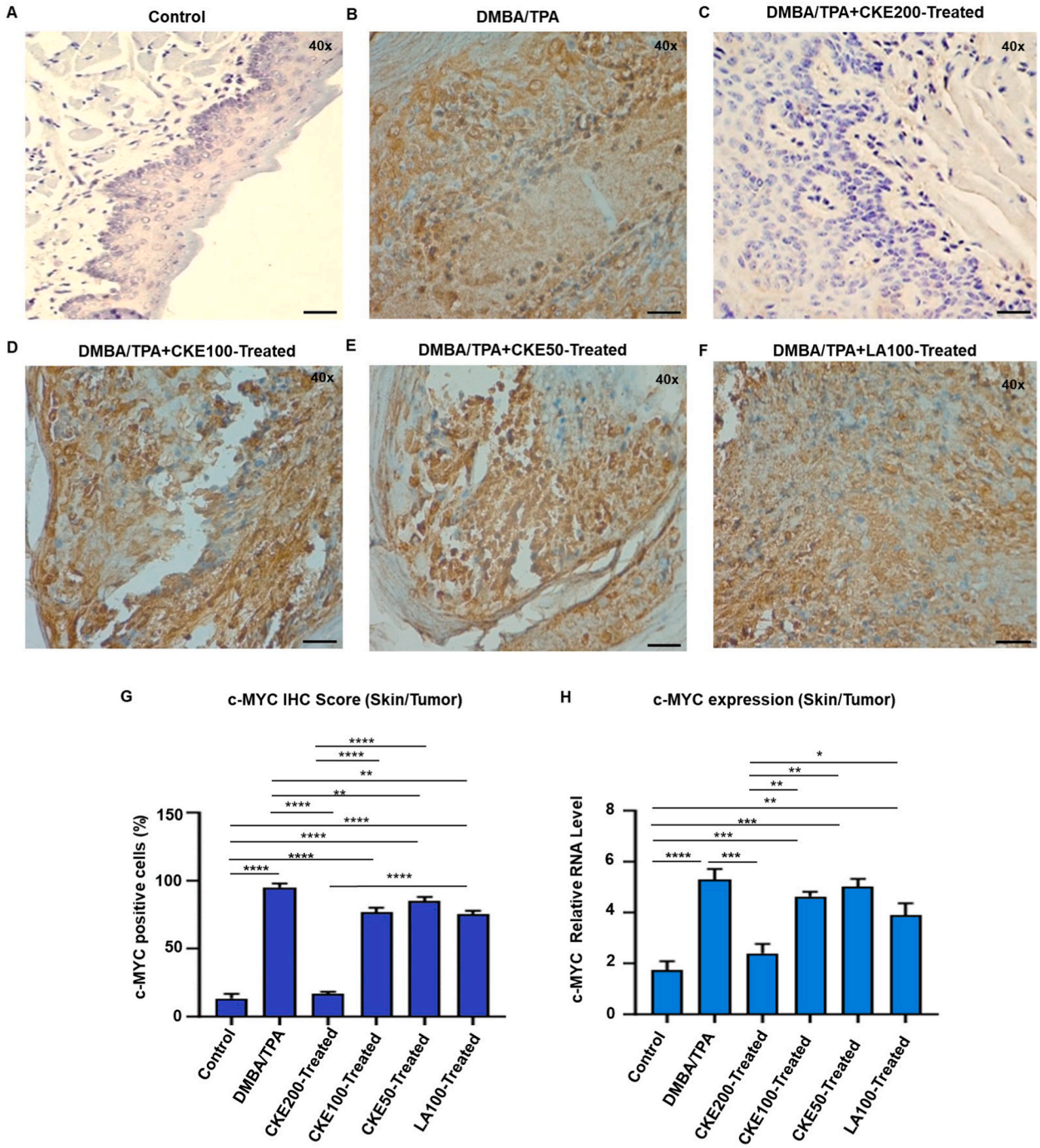

Fig. 7. IHC analysis of c-MYC expression in skin/tumors of different treatment groups at the end of 15 weeks (40× magnification). Regarding the expression of the c-MYC protein, blue indicates negative expression and brown indicates positive. **A & C.** Control and CKE200 treated groups showing strong negative (blue) staining of c-MYC protein in normal appearing cells. **B, D, E & F.** Representative images of DMBA/TPA, CKE100, CKE50, and LA100 treated groups showing scattered positive (brown) staining of c-MYC protein in tumor cells. Scale bar-20 μm **G.** Bar graph showing c-MYC IHC score based on percentage of positive (brown) cells of each grouped mice. **H.** Bar diagram showing c-MYC relative RNA levels of each grouped mice. Data are expressed as mean (N = 3) ± Standard error of mean (SEM), *p < 0.05, **p < 0.01, ***p < 0.001, ****p < 0.0001, one-way ANOVA analysis. (For interpretation of the references to colour in this figure legend, the reader is referred to the Web version of this article.)

treatment failure [61]. Additionally, drug resistance in tumors makes them difficult to treat [84–86]. Consequently, research on naturally occurring anticancer or chemopreventive drugs are receiving increased attention. Therefore, as indicated in Fig. 2A, we first isolated CKE from CK using conventional methods and then put it through a characterization procedure in an effort to find a potent, non-toxic, dietary product-based anticancer drug with high antioxidant properties from easily accessible food sources. Identification of major bioactive compound contained in CKE, its in vitro antioxidant capacity based on DPPH, H_2O_2, TPC and TFC analysis, and its potential for acute toxicity in vivo are all evaluated during the characterization process. The presence of LA in CKE was verified by HPLC analysis (Fig. 2B), and its chemical structure was revealed by ^{1}HNMR (Fig. 2C & D) and ^{13}CNMR (Supplementary Fig. 1B). Additionally, we found that CKE significantly outperforms ascorbic acid in terms of antioxidant potential (****$P < 0.0001$, DPPH, Fig. 2E; *$P < 0.05$, H_2O_2, Fig. 2F). CEK also exhibits high TPC and TFC (Fig. 2G). According to these findings, there may be a correlation between the antioxidant activity and phenolic/flavonoid compounds of CKE, as suggested by yeni et al., 2021 and Leliana et al., 2022 [74,75]. Moreover, during in vivo acute oral toxicity studies, CKE demonstrated non-toxicity up to 2000 mg/kg body weight in mice. These findings implied that CKE is a naturally occurring antioxidant that is not harmful to the body.

Further, in order to explore a potent natural antioxidant-based anticancer drug, we have chosen to study the entire extract of CK (CKE), which is a combination of numerous compounds present in CKE, rather than focusing on a single compound. In this regard, a study demonstrated that combining naturally occurring inhibitors as blocking and suppressing agents in cancer chemoprevention treatment against DMBA-induced mammary tumors was more effective than single-agent treatment [87]. Moreover, a few compounds found in VCO have been reported to already exhibit anticancer activity. For example, LA, a medium-chain saturated fatty acid (MCFA) found in coconut oil (also found in human breast milk, approximately 6.2 % of total fat [72], induces apoptosis in colon cancer (Caco-2 and IEC-6) cells by modifying glutathione levels and cell cycle phases [88]. Similarly, Coconut oil's short-chain saturated fatty acids (SCFA), including capric, caproic, and caprylic acids, have shown significant anticancer effects on human colorectal cancer (HCT-116), breast cancer (MDA-MB-231) and skin cancer (A-431) cell lines [89]. Moreover, scientific evidence shows that coconut oil, when added to the diets of lab animals induced with chemically induced cancer, can completely negate carcinogenic effects [90,91]. Thus, according to the aforementioned reports, coconuts are rich in compounds that exhibit anticancer properties. Therefore, together, these compounds may serve as potent anticancer agents by preventing or inhibiting tumor growth at various stages. Additionally, we employed standard LA as a positive control for the CKE. We have set the LA dosage at 100 mg/kg of mice body weight in order to make it comparable to Group III (CKE200, the group that received 200 mg/kg of mice body weight). Since reports suggested that approximately 50 % of lauric acid is present in coconut oil [28,72,92].

The study revealed a significant decrease in body weight in DMBA/TPA-induced mice compared to control and CKE-treated groups, with a dose-dependent decrease observed in the CKE50, CKE100, and CKE200 groups (Fig. 3A). Surprisingly, mice in the CKE200 and control groups showed no tumor formation until the end of the experiment, while mice in the DMBA/TPA, CKE100, CKE50, LA100 treated groups did show tumor formation (Fig. 3B & Supplementary Fig. 2). However, the CKE100, CKE50, and LA100 treated groups showed fewer tumors than the mice given DMBA/TPA. Significantly, only one of the eight mice given LA100 developed two tumors, which is strikingly similar to the mice given CKE200, who did not develop any tumors in any of the individual mice. The study also confirmed SCC development in DMBA/TPA, CKE100, CKE 50, and LA100 treated mice compared to control and CKE200-treated groups. Histopathological analysis showed squamous pearls and hyperplasia in some epithelial cells in DMBA/TPA induce mice (Fig. 4B), while normal epidermal layers were observed in both CKE200-treated (Fig. 4C) and control (Fig. 4A) mice. CKE200 treatment may protect the skin epidermal layer by thinning and losing the waviness of the epidermal layer compared to control mice as shown in Fig. 4A & C. Thus, the study indicates that CKE treatment alters the epidermal layer of mice's skin, potentially inhibiting or delaying tumor formation in DMBA/TPA-induced mice, with dose-dependent effects.

To better understand the underlying cellular mechanism that helps prevent or delay tumor formation in DMBA/TPA-induced mice, we further investigate the antioxidant defense mechanism of CKE based on oxidative stress analysis. Oxidative stress disrupts ROS, contributing to carcinogenesis by affecting cellular targets like proteins, carbohydrates, and phospholipids, potentially damaging DNA or other biomolecules [93,94]. Skin has antioxidant defenses that eliminate ROS, but high UV light doses can overwhelm these defenses [95–97]. Thus, the accumulation of ROS causes a variety of skin cancers as well as other inflammatory conditions of the skin [98,99]. ROS significantly contribute to tumor initiation and promotion, enhancing metabolic activation during multistep carcinogenesis [96,100,101]. Chemically produced mouse skin tumors have been shown to have insufficient antioxidant capacity or excessive ROS production [101–103]. Similarly, we also found that significant increase oxidative stress in DMBA/TPA induce mice compare to control and CKE-treated groups. According to Deepika et al. (1999), the liver is the functional organ involved in the process of drug metabolism and detoxification [101]. Consequently, we assessed the concentration of ROS, antioxidant enzymes like GSH, SOD and CAT, and MDA, a marker of oxidative stress, in the skin, tumor and livers of mice treated with control, DMBA/TPA, and CKE/LA. Increased MDA levels are thought to encourage the growth of cancerous cells through the production of ROS [104]. In our biological system, oxidative stress produces MDA or other aldehydes that link proteins with nucleic acid. By creating cross-links between these proteins in the form of amino acids and DNA, these molecules may alter transcription and replication, which may result in the formation of tumors [101–105]. Here, we found that mice induced with DMBA/TPA had skin/tumor (Fig. 5A–E) and liver (Fig. 6A–E) with significantly increased ROS and MDA levels, and decreased GSH, SOD, and CAT levels. These findings suggest that oxidative stress is increased in these animals, which can lead to skin carcinogenesis. In contrast to DMBA/TPA-induced mice, the skin/tumor (Fig. 5A–E) and liver (Fig. 6A–E) of mice treated with CKE 200, CKE 100, CKE 50, and LA100 displayed decreased ROS and MDA levels, and increased GSH, SOD, and CAT levels, indicating CKE's oxidative stress inhibitory effect. Our findings align with the many research that have shown reduced GSH, SOD, and CAT levels in the genesis of skin cancer [100,106,107]. These findings therefore indicate that CKE supports an antioxidant-based defense mechanism that protects mice against oxidative stress and the skin carcinogenesis caused by DMBA/TPA. Most significantly, based on our findings in Figs. 3–6 indicates LA100-treated group mice is more comparable to mice

in the CK200-treated group mice.

Additionally, to explore CKE effect on c-MYC expression in DMBA/TPA induced mice, we performed IHC and qPCR analysis of Skin and tumor tissue obtained from all grouped mice. According to reports, the development of SSC is influenced by the activation of proto-oncogenes like c-MYC overexpression and/or the inactivation of tumor suppressor genes like p53 mutation (34, 40–43). c-MYC was one of the first oncogenes to be identified as being involved in the development of cancer. It was discovered that c-MYC's over-expression increased pluripotency and tumorigenicity [28]. Basic helix-loop-helix leucine zippers, or bHLH-Zip, are proteins that the MYC gene normally encodes. These proteins can control apoptosis, differentiation, and cellular proliferation [33,34]. However, aberrant expression of c-MYC results in more aggressive cell growth behaviour both in vitro and in vivo [35], which is frequently seen in human cancer [32]. Nevertheless, c-MYC activity significantly increases the development of somatic cells reprogramming into pluripotency [108] and induced pluripotent stem cells isolated from mouse embryonic and adult fibroblasts [109]. Thus, these reports implied that pluripotency, tumorigenicity, and c-MYC expression may be strongly correlated in the cases of cancer stem cells (CSCs) and embryonic stem cells (ESCs) [108]. Accordingly, c-MYC activation has come to be recognized as a marker for the start and continuation of carcinogenesis [110]. Our IHC (Fig. 7A–F) and qPCR (Fig. 7G) results showed significant increased expression of c-MYC protein in the skin/tumor of mice treated with DMBA/TPA, CKE100, CKE50, and LA100, and significant decreased c-MYC expression in control (Fig. 7A) and CKE200-treated (Fig. 7C) mice. Thus, we concluded that CKE might inhibit the c-MYC gene; however, since the c-MYC gene was expressed positively in mice treated with CKE100 and CKE50 (Fig. 7D & E), the dosage of CKE needs to be increased in order to inhibit the c-MYC gene.

Taken together, our results showed that c-MYC mediated oxidative stress in DMBA/TPA induced mice. Since it has been reported that c-MYC act as inducer for ROS generation and DNA damage, and the regulation of ROS homeostasis is control by c-MYC activity in the cells [47,48,110]. Consequently, CKE may prevent skin cancer progression by modulating c-MYC mediated oxidative stress induced by DMBA/TPA. However, larger clinical intervention studies such as the long-term effect of CKE dosage on weight loss, cardiovascular disease, total and low-density lipoprotein (LDL) cholesterol, oxidative stress etc. based on in vitro and in vivo studies required before implementing CKE for clinical application [111–116].

5. Conclusion

The study investigated the effects of CKE on oxidative stress, C-MYC proto-oncogene, and tumor formation in a skin cancer model induced by DMBA/TPA. LA found to be major component in CKE. CKE exhibits invitro antioxidant activity. CKE treatment significantly inhibited tumor development by reducing c-MYC expression and modulating oxidative stress induced by DMBA/TPA. Thus, CKE acts as a dietary potent antioxidant and c-MYC inhibitor by modulating c-MYC mediated oxidative stress brought on by DMBA/TPA, that delays or prevents mouse skin from skin cancer. However, the observation of the c-MYC protein expression level in normal skin represents a significant technical limitation of the study. Since all skin tissue obtained from CKE and LA treated groups except the DMBA/TPA treated group showed negative expression of the c-MYC protein while all tumor tissue demonstrated strong positive expression of the protein. Thus, for the CKE treatment for skin cancer to be clinically successful, more pre-clinical research is required.

Data availability statement

Data included in article/supp. material/referenced in article.

Ethics statement

All protocols related to animal experimentation have been approved by Gauhati University's Institutional Animal Ethics Committee (IAEC) (IAEC/PER/2014–2015/02).

Funding statement

The experimental work was supported by Department of Bioengineering and Technology, Gauhati University, Guwahati, Assam and Kavikrisna Laboratory (Non-government organization), Indian institute of Technology (IIT)-Guwahati, Guwahati, Assam in the form of financial assistance to carry out this study. For fellowship support, Sorra Sandhya is grateful to the Indian Council of Medical Research (ICMR)-Research Associate (RA)-III fellowship (45/11/2020-DDI/BMS).

CRediT authorship contribution statement

Sorra Sandhya: Writing – original draft, Validation, Methodology, Investigation, Formal analysis. **Joyeeta Talukdar:** Writing – original draft, Validation, Investigation, Formal analysis. **Gayatri Gogoi:** Validation, Methodology, Investigation, Formal analysis. **Kumar Saurav Dey:** Writing – original draft, Methodology, Investigation, Formal analysis. **Bikul Das:** Writing – review & editing, Supervision, Project administration, Methodology, Investigation, Funding acquisition, Formal analysis, Conceptualization. **Debabrat Baishya:** Writing – review & editing, Validation, Supervision, Project administration, Investigation, Formal analysis, Conceptualization.

Declaration of competing interest

The authors of this manuscript declares there is no conflict of interest.

Acknowledgements

The authors sincerely thank Prof. Chandana Choudhury Barua of the Assam Veterinary Science College's Department of Pharmacology for her invaluable guidance during the acute oral toxicity study. The authors would like to express their gratitude to Dr. Bula Choudhury, a senior scientist. The Animal House facility of Gauhati University's Zoology department in Guwahati, Assam, and the Sophisticated Analytical Instrument Facility of Indian Institute of Technology (IIT) in Guwahati, Assam, for NMR analysis are also acknowledged by the authors.

Abbreviations

A-431	Skin Cancer Cell Line
BCC	Basal Cell Carcinoma
BSA	Bovine Serum Albumin
BSI	Botanical Survey of India
Caco-2	Colon Cancer Cell Line
CAT	Catalase
CSCs	Cancer Stem Cells (CSCs)
CK	Coconut Kernel
CKE	Coconut Kernel Extract
CKE50	50mgCKE/kg body weight of mice
CKE100	100mgCKE/kg body weight of mice
CKE200	200mgCKE/kg body weight of mice
DMBA	7,12-Dimethylbenz(a)anthracene
DNA	Deoxyribonucleic Acid
DPPH	2, 2-diphenyl-1-picrylhydrazyl
DTNB	N-butanol-pyridine, 5,5′-dithiobis (2-nitrobenzoic acid)
EDTA	Ethylene-diamine-tetra acetic acid
FBS	Foetal Bovine Serum
GPx	Glutathione Peroxidase
GSH	Glutathione
GR	L-Glutathione, reduced HCT-116: Colorectal Cancer Cell Line
H & E	Hematoxylin and Eosin (H&E)
H_2O_2	Hydrogen peroxide
HPLC	High Performance Liquid Chromatography
IAEC	Institutional Animal Ethics Committee
IEC-6	Colon Cancer Cell Line
IHC	Immunohistochemistry
IIT	Indian Institute of Technology
LA	Lauric Acid
LDL	Low-density Lipoprotein
MDA	Lipid Peroxidation
MCFA	Medium-chain Saturated Fatty Acid
NaCl	Sodium Chloride
Na_2HPO_4	Sodium Phosphate
NMR	Nuclear Magnetic Resonance
NMSC	Non-melanoma Skin Cancer
ROS	Reactive Oxygen Species
SCC	Squamous Cell Carcinoma (SCC)
SOD	Superoxide Dismutase
SCFA	Short-chain Saturated Fatty Acids
TPA	12-*O*-tetradecanoylphorbol-13-acetate
UV	Ultraviolet
VCO	Virgin Coconut Oil

Appendix A. Supplementary data

Supplementary data to this article can be found online at https://doi.org/10.1016/j.heliyon.2024.e29385.

References

[1] V. Samarasinghe, V. Madan, Nonmelanoma skin cancer, J. Cutan. Aesthetic Surg. 5 (1) (2012) 3–10, https://doi.org/10.4103/0974-2077.94323. PMID: 22557848; PMCID: PMC3339125.

[2] N.H. Khan, M. Mir, L. Qian, M. Baloch, M.F. Ali Khan, A.U. Rehman, E.E. Ngowi, D.D. Wu, X.Y. Ji, Skin cancer biology and barriers to treatment: recent applications of polymeric micro/nanostructures, J. Adv. Res. 16 (36) (2021) 223–247, https://doi.org/10.1016/j.jare.2021.06.014. PMID: 35127174; PMCID: PMC8799916.

[3] H. Sung, J. Ferlay, R.L. Siegel, M. Laversanne, I. Soerjomataram, A. Jemal, F. Bray, Global cancer Statistics 2020: GLOBOCAN estimates of incidence and mortality worldwide for 36 cancers in 185 Countries, CA Cancer J. Clin. 71 (3) (2021) 209–249, https://doi.org/10.3322/caac.21660. Epub 2021 Feb 4. PMID: 33538338.

[4] A. Combalia, C. Carrera, Squamous cell carcinoma: an update on diagnosis and treatment, Dermatol. Pract. Concept. 10 (3) (2020) e2020066, https://doi.org/10.5826/dpc.1003a66. PMID: 32642314; PMCID: PMC7319751.

[5] M. Alam, D. Ratner, Cutaneous squamous-cell carcinoma, N. Engl. J. Med. 344 (13) (2001) 975–983, https://doi.org/10.1056/NEJM200103293441306. PMID: 11274625.

[6] D. Didona, G. Paolino, U. Bottoni, C. Cantisani, NonMelanoma skin cancer pathogenesis overview, Biomedicines 6 (1) (2018) 6, https://doi.org/10.3390/biomedicines6010006. PMID: 29301290; PMCID: PMC5874663.

[7] U. Leiter, T. Eigentler, C. Garbe, Epidemiology of skin cancer, Adv. Exp. Med. Biol. 8 (10) (2014) 120–140, https://doi.org/10.1007/978-1-4939-0437-2_7. PMID: 25207363.PMID: 23877569.

[8] N. Eisemann, A. Waldmann, A.C. Geller, M.A. Weinstock, B. Volkmer, R. Greinert, E.W. Breitbart, A. Katalinic, Non-melanoma skin cancer incidence and impact of skin cancer screening on incidence, J. Invest. Dermatol. 134 (1) (2014) 43–50, https://doi.org/10.1038/jid.2013.304. Epub 2013 Jul 22. PMID: 23877569.

[9] M.J. Eide, R. Krajenta, D. Johnson, J.J. Long, G. Jacobsen, M.M. Asgari, H.W. Lim, C.C. Johnson, Identification of patients with nonmelanoma skin cancer using health maintenance organization claims data, Am. J. Epidemiol. 171 (1) (2010) 123–128, https://doi.org/10.1093/aje/kwp352. Epub 2009 Dec 6. PMID: 19969529; PMCID: PMC2796985.

[10] U. Leiter, U. Keim, C. Garbe, Epidemiology of skin cancer: update 2019, Adv. Exp. Med. Biol. 1268 (2020) 123–139, https://doi.org/10.1007/978-3-030-46227-7_6. PMID: 32918216.

[11] G. Khullar, U. Saikia, B. Radotra, Nonmelanoma skin cancers: an Indian perspective, Indian Journal of Dermatopathology and Diagnostic Dermatology 1 (2) (2014) 55–62, https://doi.org/10.4103/2349-6029.147282.

[12] V. Samarasinghe, V. Madan, J.T. Lear, Management of high-risk squamous cell carcinoma of the skin, Expert Rev. Anticancer Ther. 11 (5) (2011) 763–769, https://doi.org/10.1586/era.11.36. PMID: 21554051.

[13] J. Garcia-Zuazaga, S.M. Olbricht, Cutaneous squamous cell carcinoma, Adv. Dermatol. 24 (2008) 33–57, https://doi.org/10.1016/j.yadr.2008.09.007. PMID: 19256304.

[14] A.P. Marco, S. Gabriella, M.C. Carlo, Oncogenes in the initiation and progression of neoplasia, in: W. Donald, R.E.P. Kufe, Ralph R. Weichselbaum, Robert C. Bast Jr, S Gansler Ted, James F. Holland, Emil Frei (Eds.), Holland-frei Cancer Medicine, sixth ed. ed, 2003.

[15] Y.H. Kong, S.P. Xu, Salidroside prevents skin carcinogenesis induced by DMBA/TPA in a mouse model through suppression of inflammation and promotion of apoptosis, Oncol. Rep. 39 (6) (2018) 2513–2526, https://doi.org/10.3892/or.2018.6381. Epub 2018 Apr 18. PMID: 29693192; PMCID: PMC5983924.

[16] J. Goldstein, E. Roth, N. Roberts, R. Zwick, S. Lin, S. Fletcher, A. Tadeu, C. Wu, A. Beck, C. Zeiss, M. Suárez-Fariñas, V. Horsley, Loss of endogenous Nfatc1 reduces the rate of DMBA/TPA-induced skin tumorigenesis, Mol. Biol. Cell 26 (20) (2015) 3606–3614, https://doi.org/10.1091/mbc.E15-05-0282. Epub 2015 Aug 26. PMID: 26310443; PMCID: PMC4603931.

[17] Y. Bai, H. Edamatsu, S. Maeda, H. Saito, N. Suzuki, T. Satoh, T. Kataoka, Crucial role of phospholipase Cepsilon in chemical carcinogen-induced skin tumor development, Cancer Res. 64 (24) (2004) 8808–8810, https://doi.org/10.1158/0008-5472.CAN-04-3143. PMID: 15604236.

[18] M. Vabeiryureilai, K. Lalrinzuali, G.C. Jagetia, Chemopreventive effect of hesperidin, a citrus bioflavonoid in two stage skin carcinogenesis in Swiss albino mice, Heliyon 5 (10) (2019) e02521, https://doi.org/10.1016/j.heliyon.2019.e02521. PMID: 31720442; PMCID: PMC6838872.

[19] M. DebMandal, S. Mandal, Coconut (Cocos nucifera L.: Arecaceae): in health promotion and disease prevention, Asian Pac. J. Tropical Med. 4 (3) (2011) 241–247, https://doi.org/10.1016/S1995-7645(11)60078-3. Epub 2011 Apr 12. PMID: 21771462.

[20] S. Sandhya, J. Talukdar, G. Gogoi, H. Li, D. Baishya, B. Das, Coconut kernel extract as a novel chemopreventive agent that target cancer stemness [abstract], 79 (13 Suppl), in: Proceedings of the American Association for Cancer Research Annual Meeting 2019; Atlanta, GA. Philadelphia (PA): AACR; Cancer Res, 2019. Abstract nr 1614.

[21] H. Kumudini, J. Shaveen, Coconut oil: it's good for you after all. Report. https://www.sundaytimes.lk/111016/Plus/plus_05.html, 2011.

[22] F.A. Sinaga, U. Harahap, J. Silalahi, H. Sipahutar, Antioxidant effect of virgin coconut oil on urea and creatinine levels on maximum physical activity, open access maced, J. Med. Sci. 7 (22) (2019) 3781–3785, https://doi.org/10.3889/oamjms.2019.503. PMID: 32127975; PMCID: PMC7048370.

[23] X. Chen, D.I. Kim, H.G. Moon, M. Chu, K. Lee, Coconut oil alleviates the oxidative stress-mediated inflammatory response via regulating the MAPK pathway in particulate matter-stimulated alveolar macrophages, Molecules 29 (9) (2022) 2898, https://doi.org/10.3390/molecules27092898. PMID: 35566249; PMCID: PMC9105152.

[24] N.A. Kamalaldin, S.A. Sulaiman, A. Seeni, B.H. Yahaya, Virgin coconut oil (VCO) inhibits cell growth via apoptosis on lung cancer cell lines, The Open Conference Proccedings Journal 4 (290) (2013) 202, https://doi.org/10.2174/2210289201304010290.

[25] Y. Badrul, S. Siti Amrah, Y. Rahimi, Apoptosis in lung cancer cells induced by virgin cocnut oil, Regenerative Research 4 (2015) (2015) 1–7.

[26] P. Verma, S. Naik, P. Nanda, S. Banerjee, S. Naik, A. Ghosh, In vitro anticancer activity of virgin coconut oil and its fractions in liver and oral cancer cells, anticancer agents med, Chem 19 (18) (2019) 2223–2230, https://doi.org/10.2174/1871520619666191021160752. PMID: 31736449.

[27] F.P.K. Lim, L.F.G. Bongosia, N.B.N. Yao, L.A. Santiago, Cytotoxic activity of the phenolic extract of virgin coconut oil on human hepatocarcinoma cells (HepG2), Int. Food Res. J. 21 (2) (2014) 729–733.

[28] V. Ramya, K.P. Shyam, E. Kowsalya, C.K. Balavigneswaran, B. Kadalmani, Dual roles of coconut oil and its major component lauric acid on redox nexus: focus on cytoprotection and cancer cell death, Front. Neurosci. 11 (16) (2022) 833630, https://doi.org/10.3389/fnins.2022.833630. PMID: 35360165; PMCID: PMC8963114.

[29] J.K. Fauser, G.M. Matthews, A.G. Cummins, G.S. Howarth, Induction of apoptosis by the medium-chain length fatty acid lauric acid in colon cancer cells due to induction of oxidative stress, Chemotherapy 59 (3) (2013) 214–224, https://doi.org/10.1159/000356067. Epub 2013 Dec 13. PMID: 24356281.

[30] A. Namachivayam, A. Valsala Gopalakrishnan, Effect of Lauric acid against ethanol-induced hepatotoxicity by modulating oxidative stress/apoptosis signalling and HNF4α in Wistar albino rats, Heliyon 9 (11) (2023) e21267, https://doi.org/10.1016/j.heliyon.2023.e21267. PMID: 37908709; PMCID: PMC10613920.

[31] P.S. Knoepfler, Deconstructing stem cell tumorigenicity: a roadmap to safe regenerative medicine, Stem Cell. 27 (5) (2009) 1050–1056, https://doi.org/10.1002/stem.37. PMID: 19415771; PMCID: PMC2733374.

[32] K.M. Greulich, J. Utikal, R.U. Peter, G. Krähn, c-MYC and nodular malignant melanoma. A case report, Cancer 89 (1) (2000) 97–103, https://doi.org/10.1002/1097-0142(20000701)89:1<97::aid-cncr14>3.0.co;2-0. PMID: 10897006.

[33] B.L. Amati, H, Myc-Max-Mad: a transcription factor network controlling cell cycle progression, differentiation and death, Curr. Opin. Genet. Dev. 4 (1) (1994) 102–108, https://doi.org/10.1016/0959-437x(94)90098-1. PMID: 8193530.

[34] S. Pelengaris, T. Littlewood, M. Khan, G. Elia, G. Evan, Reversible activation of c-Myc in skin: induction of a complex neoplastic phenotype by a single oncogenic lesion, Mol. Cell. 3 (5) (1999) 565–577, https://doi.org/10.1016/s1097-2765(00)80350-0. PMID: 10360173.

[35] H. Schlagbauer-Wadl, M. Griffioen, A. van Elsas, P.I. Schrier, T. Pustelnik, H.G. Eichler, K. Wolff, H. Pehamberger, B. Jansen, Influence of increased c-Myc expression on the growth characteristics of human melanoma, J. Invest. Dermatol. 112 (3) (1999) 332–336, https://doi.org/10.1046/j.1523-1747.1999.00506.x. PMID: 10084311.

[36] G. Donati, B. Amati, MYC and therapy resistance in cancer: risks and opportunities, Mol. Oncol. 16 (21) (2022) 3828–3854, https://doi.org/10.1002/1878-0261.13319. Epub 2022 Oct 20. PMID: 36214609; PMCID: PMC9627787.

[37] M.J. Duffy, S. O'Grady, M. Tang, J. Crown, MYC as a target for cancer treatment, Cancer Treat Rev. 94 (2021) 102154, https://doi.org/10.1016/j.ctrv.2021.102154. Epub 2021 Jan 19. PMID: 33524794.

[38] C. Wang, J. Zhang, J. Yin, Y. Gan, S. Xu, Y. Gu, W. Huang, Alternative approaches to target Myc for cancer treatment, Signal Transduct. Target Ther. 6 (1) (2021) 117, https://doi.org/10.1038/s41392-021-00500-y. PMID: 33692331; PMCID: PMC7946937.

[39] H. Chen, H. Liu, G. Qing, Targeting oncogenic Myc as a strategy for cancer treatment, Signal Transduct. Targeted Ther. 3 (2018) 5, https://doi.org/10.1038/s41392-018-0008-7. PMID: 29527331; PMCID: PMC5837124.

[40] P. Boukamp, Non-melanoma skin cancer: what drives tumor development and progression? Carcinogenesis 26 (10) (2005) 1657–1667, https://doi.org/10.1093/carcin/bgi123. Epub 2005 May 19. PMID: 15905207.

[41] H. Nakazawa, D. English, P.L. Randell, K. Nakazawa, N. Martel, B.K. Armstrong, H. Yamasaki, UV and skin cancer: specific p53 gene mutation in normal skin as a biologically relevant exposure measurement, Proc. Natl. Acad. Sci. U.S.A. 91 (1) (1994) 360–364, https://doi.org/10.1073/pnas.91.1.360. PMID: 8278394; PMCID: PMC42947.

[42] T. Oskarsson, M.A. Essers, N. Dubois, S. Offner, C. Dubey, C. Roger, D. Metzger, P. Chambon, E. Hummler, P. Beard, A. Trumpp, Skin epidermis lacking the c-Myc gene is resistant to Ras-driven tumorigenesis but can reacquire sensitivity upon additional loss of the p21Cip1 gene, Genes Dev. 20 (15) (2006) 2024–2029, https://doi.org/10.1101/gad.381206. PMID: 16882980; PMCID: PMC1536054.

[43] Z. Zhang, R. Yao, J. Li, Y. Wang, C.W. Boone, R.A. Lubet, M. You, Induction of invasive mouse skin carcinomas in transgenic mice with mutations in both H-ras and p53, Mol. Cancer Res. 3 (10) (2005) 563–574, https://doi.org/10.1158/1541-7786.MCR-05-0144. PMID: 16254190.

[44] B. Das, B. Pal, R. Bhuyan, H. Li, A. Sarma, S. Gayan, J. Talukdar, S. Sandhya, S. Bhuyan, G. Gogoi, A.M. Gouw, D. Baishya, J.R. Gotlib, A.C. Kataki, D. W. Felsher, MYC regulates the HIF2α stemness pathway via nanog and Sox2 to maintain self-renewal in cancer stem cells versus non-stem cancer cells, Cancer Res. 79 (16) (2019) 4015–4025, https://doi.org/10.1158/0008-5472.CAN-18-2847. Epub 2019 Jul 2. PMID: 31266772; PMCID: PMC6701948.

[45] S.B. McMahon, MYC and the control of apoptosis, Cold Spring Harb Perspect Med 4 (7) (2014) a014407, https://doi.org/10.1101/cshperspect.a014407. PMID: 24985130; PMCID: PMC4066641.

[46] N. Denis, A. Kitzis, J. Kruh, F. Dautry, D. Corcos, Stimulation of methotrexate resistance and dihydrofolate reductase gene amplification by c-myc, Oncogene 6 (8) (1991) 1453–1457. PMID: 1886715.

[47] O. Vafa, M. Wade, S. Kern, M. Beeche, T.K. Pandita, G.M. Hampton, G.M. Wahl, c-Myc can induce DNA damage, increase reactive oxygen species, and mitigate p53 function: a mechanism for oncogene-induced genetic instability, Mol. Cell 9 (5) (2002) 1031–1044, https://doi.org/10.1016/s1097-2765(02)00520-8. PMID: 12049739.

[48] J.A. Graves, M. Metukuri, D. Scott, K. Rothermund, E.V. Prochownik, Regulation of reactive oxygen species homeostasis by peroxiredoxins and c-Mice, J. Biol. Chem. 284 (10) (2009) 6520–6529, https://doi.org/10.1074/jbc.M807564200. Epub 2008 Dec 19. PMID: 19098005; PMCID: PMC2649099.

[49] A.A. Anzaku, J.I. Akyala, A. Juliet, E.C. Obianuju, Antibacterial activity of lauric acid on some selected clinical isolates, Ann. Clin. Lab. Res. 5 (2) (2017) 1–5.

[50] M. Kanno, Analysis of Fatty Acids in Rice Bran Oil, Coconut Oil and Margarine by HPLC-ELSD. https://jascoinc.com/applications/analysis-of-fatty-acids-in-rice-bran-oil-coconut-oil-and-margarine-by-hplc-elsd/..

[51] S. Sandhya, Identification of potent herbal chemopreventive agent. PhD thesis, Gauhati University. http://hdl.handle.net/10603/199165..

[52] S. Parthasarathy, J. Bin Azizi, S. Ramanathan, S. Ismail, S. Sasidharan, M.I. Said, S.M. Mansor, Evaluation of antioxidant and antibacterial activities of aqueous, methanolic and alkaloid extracts from Mitragyna speciosa (Rubiaceae family) leaves, Molecules 14 (10) (2009) 3964–3974.

[53] S.D. Kumar, K.G. Surajit, S. Sorra, T. Joyeeta, S. Dipankar, Assessment of in vitro antioxidant potential and in vivo anti-diabetic activity on streptozotocin-induced diabetic rats of rumex maritimus L, Asian J. Biochem. Pharmaceut. Res. 4 (2) (2014) 64–170.

[54] R.M. Patel, N.J. Patel, In vitro antioxidant activity of coumarin compounds by DPPH, Super oxide and nitric oxide free radical scavenging methods, J. Adv. Pharm. Educ. Res. 1 (2011) 52–68.

[55] D.N. Kaur, N.P. Nain, J. Nain, In vitro antimicrobial and antioxidant activity of Ginkgo Biloba Bark Extract, Int. Res. J. Pharm. 3 (6) (2012) 116–119.

[56] I. Gulcin, O.L. Kufrevioglu, M. Oktay, M.E. Buyukokuroglu, Antioxidant, antimicrobial, antiulcer and analgesic activities of nettle (Urtica dioica L.), J. Ethnopharmacol. 90 (2) (2004) 205–215.

[57] N.A.A. Ghani, A.A. Channip, H.H.P. Chok, F. Ja'afar, H.M. Yasin Usman A, Physicochemical properties, antioxidant capacities, and metal contents of virgin coconut oil produced by wet and dry processes, Food Sci. Nutr. 6 (5) (2018) 1298–1306, https://doi.org/10.1002/fsn3.671. PMID: 30065831; PMCID: PMC6060898.

[58] K.A. Adekola, A.B. Salleh, U.H. Zaidan, A. Azlan, E. Chiavaro, M. Paciulli, J.M.N. Marikkar, Total phenolic content, antioxidative and antidiabetic properties of Coconut (cocos nucjfera L.) testa and selected bean seed coats, Ital. J. Food Sci. 29 (2017) 741–753.

[59] R.B. Filler, S.J. Roberts, M. Girardi, Cutaneous Two-Stage Chemical Carcinogenesis, pdb.prot4837, CSH Protoc., 2007, https://doi.org/10.1101/pdb.prot4837. PMID: 21357170.

[60] Y.H. Kong, S.P. Xu, Salidroside prevents skin carcinogenesis induced by DMBA/TPA in a mouse model through suppression of inflammation and promotion of apoptosis, Oncol. Rep. 39 (6) (2018) 2513–2526, https://doi.org/10.3892/or.2018.6381. Epub 2018 Apr 18. PMID: 29693192; PMCID: PMC5983924.

[61] B. Das, H. Yeger, H. Baruchel, M.H. Freedman, G. Koren, S. Baruchel, In vitro cytoprotective activity of squalene on a bone marrow versus neuroblastoma model of cisplatin-induced toxicity. implications in cancer chemotherapy, Eur. J. Cancer 39 (17) (2003) 2556–2565, https://doi.org/10.1016/j.ejca.2003.07.002. PMID: 14602142.

[62] F. Majed, S. Nafees, S. Rashid, N. Ali, S.K. Hasan, R. Ali, A. Shahid, S. Sultana, Terminalia chebula attenuates DMBA/Croton oil-induced oxidative stress and inflammation in Swiss albino mouse skin, Toxicol. Int. 22 (1) (2015) 21–29, https://doi.org/10.4103/0971-6580.172252. PMID: 26862256; PMCID: PMC4721172.

[63] B. Das, H. Yeger, R. Tsuchida, R. Torkin, M.F. Gee, P.S. Thorner, M. Shibuya, D. Malkin, S. Baruchel, A hypoxia-driven vascular endothelial growth factor/Flt1 autocrine loop interacts with hypoxia-inducible factor-1alpha through mitogen-activated protein kinase/extracellular signal-regulated kinase 1/2 pathway in neuroblastoma, Cancer Res. 65 (16) (2005) 7267–7275, https://doi.org/10.1158/0008-5472.CAN-04-4575. PMID: 16103078.

[64] B. Das, R. Tsuchida, D. Malkin, G. Koren, S. Baruchel, H. Yeger, Hypoxia enhances tumor stemness by increasing the invasive and tumorigenic side population fraction, Stem Cell. 26 (7) (2008) 1818–1830.

[65] M.M. Bradford, A rapid and sensitive method for the quantitation of microgram quantities of protein utilizing the principle of protein–dyebinding, Anal. Biochem. 72 (1976) 248–254.

[66] A. Namachivayam, A. Valsala Gopalakrishnan, Effect of Lauric acid against ethanol-induced hepatotoxicity by modulating oxidative stress/apoptosis signalling and HNF4α in Wistar albino rats, Heliyon 9 (11) (2023) e21267, https://doi.org/10.1016/j.heliyon.2023.e21267. PMID: 37908709; PMCID: PMC10613920.

[67] B. Das, R. Antoon, R. Tsuchida, S. Lotfi, O. Morozova, W. Farhat, D. Malkin, G. Koren, H. Yeger, S. Baruchel, Squalene selectively protects mouse bone marrow progenitors against cisplatin and carboplatin-induced cytotoxicity in vivo without protecting tumor growth, Neoplasia 10 (10) (2008) 1105–1119, https://doi.org/10.1593/neo.08466. PMID: 18813359; PMCID: PMC2546596.

[68] H. Ohkawa, et al., Assay of lipid peroxides in animal tissues by thiobarbituric acid reaction, Anal. Biochem. 95 (1979) 351–358.

[69] D. Deepika, et al., Chemopreventive effect of 49-demethyl epipodophyllotoxin on DMBA/TPA-induced mouse skin carcinogenesis, Carcinogenesis 20 (1999) 997–1003.

[70] H. Aebi, Catalase: in vitro, in: S.P. Colowick, N.O. Kaplan (Eds.), Method in Enzymology, vol. 105, Academic press, New York, 1984, pp. 121–126.

[71] G. Daniela, et al., Analysis of GSH and GSSG after derivatization with N-ethylmaleimide, Nat. Protoc. 9 (2013) 1660.

[72] S. Sandhya, J. Talukdar, D. Bhaishya, Chemical and biological properties of lauric acid: a review, J. Adv. Res. 4 (7) (2016) 1123–1128, https://doi.org/10.21474/IJAR01/952.

[73] L. Boateng, R. Ansong, W.B. Owusu, M. Steiner-Asiedu, Coconut oil and palm oil's role in nutrition, health and national development: a review, Ghana Med. J. 50 (3) (2016) 189–196. PMID: 27752194; PMCID: PMC5044790.

[74] Y.M. Muflihah, G. Gollavelli, Y.C. Ling, Correlation study of antioxidant activity with phenolic and flavonoid compounds in 12 Indonesian indigenous herbs, Antioxidants 10 (10) (2021) 1530, https://doi.org/10.3390/antiox10101530. PMID: 34679665; PMCID: PMC8533117.
[75] L. Lulum, W. Setyaningsih, M. Palma, Supriyadi, U. Santoso, Antioxidant activity of aqueous and ethanolic extracts of coconut (cocos nucifera) fruit by-products, Agronomy 12 (5) (2022) 1102, https://doi.org/10.3390/agronomy12051102.
[76] OECD guideline for testing of chemicals (acute oral toxicity – acute toxic Class method). https://www.oecd.org/chemicalsafety/risk-assessment/1948378.pdf, 2001.
[77] K. Chandra, et al., Protection against FCA induced oxidative stress induced DNA damage as a model of arthritis and in vitro anti-arthritic potential of Costus speciosus rhizome extract, International Journal of Pharmacognosy and Phytochemical Research 7 (2015) 383–389.
[78] I. Zelen, P. Djurdjevic, S. Popovic, M. Stojanovic, V. Jakovljevic, S. Radivojevic, D. Baskic, N. Arsenijevic, Antioxidant enzymes activities and plasma levels of oxidative stress markers in B-chronic lymphocytic leukemia patients, J BUON 15 (2) (2010) 330–336. PMID: 20658731.
[79] C.V. Dang, A. Le, P. Gao, MYC-induced cancer cell energy metabolism and therapeutic opportunities, Clin. Cancer Res. 15 (21) (2009) 6479–6483, https://doi.org/10.1158/1078-0432.CCR-09-0889. Epub 2009 Oct 27. PMID: 19861459; PMCID: PMC2783410.
[80] R. Beroukhim, et al., The landscape of somatic copy-number alteration across human cancers, Nature 463 (7283) (2010) 899–905, https://doi.org/10.1038/nature08822. PMID: 20164920; PMCID: PMC2826709.
[81] V. lombart, M.R. Mansour, Therapeutic targeting of "undruggable" MYC, EBioMedicine 75 (2022) 103756, https://doi.org/10.1016/j.ebiom.2021.103756. Epub 2021 Dec 20. PMID: 34942444; PMCID: PMC8713111.
[82] O. Surien, S.F. Masre, D.F. Basri A, R. Ghazali, Chemopreventive effects of oral pterostilbene in multistage carcinogenesis of skin squamous cell carcinoma mouse model induced by DMBA/TPA, Biomedicines 10 (11) (2022) 2743, https://doi.org/10.3390/biomedicines10112743. PMID: 36359262; PMCID: PMC9687295.
[83] A.P. Marco, S. Gabriella, M.C. Carlo, Oncogenes in the initiation and progression of neoplasia, in: W. Donald, R.E.P. Kufe, Ralph R. Weichselbaum, Robert C. Bast Jr, S Gansler Ted, James F. Holland, Emil Frei (Eds.), Holland-frei Cancer Medicine, sixth ed. ed, 2003.
[84] N. Amoolya, et al., Anticarcinogenic properties of medium chain fatty acids on human colorectal, skin and breast cancer cells in vitro, Int. J. Mol. Sci. 16 (2015) 5014–5027.
[85] G. Damia, et al., The pharmacological point of view of resistance to therapy in tumors, Cancer Treat Rev. 40 (2014) 909–916.
[86] C.A. Rabik, , et al.M.E. Dolan, Molecular mechanisms of resistance and toxicity associated with platinating agents, Cancer Treat Rev. 33 (2007) 9–23.
[87] I.P. Clement, et al., Combination of blocking agents and suppressing agents in cancer prevention, Carcinogenesis 12 (1991) 365–367.
[88] J.K. Fauser, et al., Induction of apoptosis by the medium-chain length fatty acid lauric acid in colon cancer cells due to induction of oxidative stress, Chemotherapy 59 (2013) 214–224.
[89] N. Amoolya, et al., Anticarcinogenic properties of medium chain fatty acids on human colorectal, skin and breast cancer cells in vitro, Int. J. Mol. Sci. 16 (2015) 5014–5027.
[90] L.M. Assunção, H.S. Ferreira, A.F. dos Santos, C.R. Cabral Jr., T.M.M.T. Florêncio, Effects of dietary coconut oil on the biochemical and anthropometric profiles of women presenting abdominal obesity, Lipids 44 (7) (2009) 593–601, 2009.
[91] N.D. Bruce Fife, The coconut oil miracle: where is the evidence?. Scientific evidence regarding coconut oil, in: Reproduced from Healthy Ways Newsletter/ Published Fall, 2011/Published by Piccadilly Books, Ltd., 2011. www.piccadillybooks.com.
[92] S. Hewlings, Coconuts and health: different chain lengths of saturated fats require different consideration, J. Cardiovasc Dev. Dis. 7 (4) (2020) 59, https://doi.org/10.3390/jcdd7040059. PMID: 33348586; PMCID: PMC7766932.Noriko NODA* and Hiro WAKASUGI**. Cancer and Oxidative Stress. JMAJ 44(12): 535–539, 2001.
[93] E. Birben, U.M. Sahiner, C. Sachesen, S. Erzurum, O. Kalayci, Oxidative stress and antioxidant defense, World Allergy Organ J 5 (1) (2012) 9–19.
[94] R.T. Narendhirakannan, M.A. Hannah, Oxidative stress and skin cancer: an overview, Indian J. Clin. Biochem. 28 (2) (2013) 110–115, 10.1007/s12291-012-0278-8. Epub 2012 Nov 23. PMID: 24426195; PMCID: PMC3613501.
[95] J.P. Kehrer, Free radicals as mediators of tissue injury and disease, Crit. Rev. Toxicol. 23 (1) (1993) 21–48, https://doi.org/10.3109/10408449309104073. PMID: 8471159.
[96] O.I. Aruoma, Nutrition and health aspects of free radicals and antioxidants, Food Chem. Toxicol. 32 (7) (1994) 671–683, https://doi.org/10.1016/0278-6915(94)90011-6. PMID: 8045480.
[97] I.R. Record, I.E. Dreosti, M. Konstantinopoulos, R.A. Buckley, The influence of topical and systemic vitamin E on ultraviolet light-induced skin damage in hairless mice, Nutr. Cancer 16 (3–4) (1991) 219–225, https://doi.org/10.1080/01635589109514160. PMID: 1775384.
[98] Y. Kawaguchi, H. Tanaka, T. Okada, H. Konishi, M. Takahashi, M. Ito, J. Asai, The effects of ultraviolet A and reactive oxygen species on the mRNA expression of 72-kDa type IV collagenase and its tissue inhibitor in cultured human dermal fibroblasts, Arch. Dermatol. Res. 288 (1) (1996) 39–44, https://doi.org/10.1007/BF02505041. PMID: 8750933.
[99] B. Halliwell, Oxidative stress and cancer: have we moved forward? Biochem. J. 401 (1) (2007) 1–11, https://doi.org/10.1042/BJ20061131.
[100] D. Deepika, et al., Chemopreventive effect of 49-demethyl epipodophyllotoxin on DMBA/TPA-induced mouse skin carcinogenesis, Carcinogenesis 20 (1999) 997–1003.
[101] M. Athar, Oxidative stress and experimental carcinogenesis, Indian J. Exp. Biol. 40 (2002) 656–667.
[102] G. Chaudhary, Inhibition of dimethylebenz (a) anthracene (DMBA)/croton oil induced skin tumorigenesis in Swiss albino mice by Aloe veratreatment, Int. J. Biol. Med. Res. 2 (3) (2011) 671–678.
[103] L.M. Alias, et al., Protective effect of ferulic acid on 7,12-dimethylbenz[a]anthracene-induced skin carcinogenesis in Swissalbino mice, Exp. Toxicol. Pathol. 61 (2009) 205–214.
[104] L. Vellaichamy, S. Balakrishnan, K. Panjamurthy, S. Manoharan, L.M. Alias, Chemopreventive potential of piperine in 7,12-dimethylbenz[a]anthracene-induced skin carcinogenesis in Swiss albino mice, Environ. Toxicol. Pharmacol. 28 (2009) 11–18.
[105] F.L. Chung, H.J.C. Chen, R.G. Nath, Lipid peroxidation as a potentialendogenous source for the formation of exocyclic DNA adducts, J. Carcinoge. 17 (10) (1996) 2105–2111.
[106] J.P. Perchellet, M. Perchellet, Antioxidant and multistagecarcinogenesis in mouse skin, Free Radical Biol. Med. 7 (1989) 377–408.
[107] K. Takahashi, S. Yamanaka, Induction of pluripotent stem cells from mouse embryonic and adult fibroblast cultures by defined factors, Cell 126 (4) (2006) 663–676, https://doi.org/10.1016/j.cell.2006.07.024.
[108] M. Gabay, Y. Li, D.W. Felsher, MYC activation is a hallmark of cancer initiation and maintenance, Cold Spring Harb Perspect Med 4 (6) (2014), https://doi.org/10.1101/cshperspect.a014241.
[109] C. Hadjimichael, K. Chanoumidou, N. Papadopoulou, P. Arampatzi, J. Papamatheakis, A. Kretsovali, Common stemness regulators of embryonic and cancer stem cells, World J Stem Cells 7 (9) (2015) 1150–1184, https://doi.org/10.4252/wjsc.v7.i9.1150. PMID: 26516408; PMCID: PMC4620423.
[110] G. Wu, T. Liu, H. Li, Y. Li, D. Li, W. Li, c-MYC and reactive oxygen species play roles in tetrandrine-induced leukemia differentiation, Cell Death Dis. 9 (5) (2018) 473, https://doi.org/10.1038/s41419-018-0498-9. PMID: 29700286; PMCID: PMC5920096.
[111] T.C. Wallace, Health effects of coconut oil-A narrative review of current evidence, J. Am. Coll. Nutr. 38 (2) (2019) 97–107, https://doi.org/10.1080/07315724.2018.1497562. Epub 2018 Nov 5. PMID: 30395784.
[112] N. Neelakantan, J.Y.H. Seah, R.M. van Dam, The effect of coconut oil consumption on cardiovascular risk factors: a systematic review and meta-analysis of clinical trials, Circulation 141 (10) (2020) 803–814, https://doi.org/10.1161/CIRCULATIONAHA.119.043052. Epub 2020 Jan 13. PMID: 31928080.
[113] A.C. Duarte, et al., The effects of coconut oil on the cardiometabolic profile: a systematic review and meta-analysis of randomized clinical trials, Lipids Health Dis. 21 (1) (2022) 83, https://doi.org/10.1186/s12944-022-01685-z. PMID: 36045407; PMCID: PMC9429773.

[114] C.E. Vogel, L. Crovesy, E.L. Rosado, M. Soares-Mota, Effect of coconut oil on weight loss and metabolic parameters in men with obesity: a randomized controlled clinical trial, Food Funct. 11 (7) (2020) 6588–6594, https://doi.org/10.1039/d0fo00872a. Epub 2020 Jul 10. PMID: 32648861.
[115] E. Mansouri, et al., Effects of virgin coconut oil consumption on serum brain-derived neurotrophic factor levels and oxidative stress biomarkers in adults with metabolic syndrome: a randomized clinical trial, Nutr. Neurosci. (2023) 1–12, https://doi.org/10.1080/1028415X.2023.2223390. Epub ahead of print. PMID: 37409587.
[116] L. Schwingshackl, S. Schlesinger, Coconut oil and cardiovascular disease risk, Curr Atheroscler Rep 25 (5) (2023) 231–236, https://doi.org/10.1007/s11883-023-01098-y. Epub 2023 Mar 27. PMID: 36971981; PMCID: PMC10182109.